PRELIMINARY THERMAL MODELING OF HI-STORM 100S-218 VERSION B STORAGE MODULES AT HOPE CREEK NUCLEAR POWER STATION ISFSI

Fuel Cycle Research & Development

Prepared for
U.S. Department of Energy
Used Fuel Disposition Campaign

JM Cuta
HE Adkins
August 30, 2013
FCRD-UFD-2013-000297
PNNL-22552

Reviewed by:

PNNL Project Manager

Signature on file

_____

Brady Hanson

SUMMARY

This report fulfills the M3 milestone M3FT-13PN0810022, "Report on Inspection 1", under Work Package FT-13PN081002.

Thermal analysis is being undertaken at Pacific Northwest National Laboratory (PNNL) in support of inspections of selected storage modules at various locations around the United States, as part of the Used Fuel Disposition Campaign of the U.S. Department of Energy, Office of Nuclear Energy (DOE-NE) Fuel Cycle Research and Development. This report documents pre-inspection predictions of temperatures for four modules at the Hope Creek Nuclear Generating Station ISFSI that have been identified as candidates for inspection in late summer or early fall/winter of 2013. These are HI-STORM 100S-218 Version B modules storing BWR 8x8 fuel in MPC-68 canisters.

The temperature predictions reported in this document were obtained with detailed COBRA-SFS models of these four storage systems, with the following boundary conditions and assumptions.

- Individual assembly and total decay heat loadings for each canister, provided by PSEG Nuclear Fuels, based on ORIGEN modeling and a parallel set of values obtained using the methodology endorsed by RG 3.54.
- Axial decay heat distributions based on typical generic profiles for BWR fuel.
- Ambient conditions of still air at 80°F (27°C), with additional evaluations for selected modules at 90°F (32°C), 70°F (21°C), and 50°F (10°C), to cover a range of possible conditions at the time of the inspection.

All calculations are for steady-state conditions, on the assumption that the surfaces of the module that are accessible for temperature measurements during the inspection will tend to follow ambient temperature changes relatively closely.

Comparisons to the results of the inspections, and post-inspection evaluations of temperature measurements obtained in the specific modules, will be documented in a separate follow-on report, to be issued in a timely manner after the inspection has been performed.

ACKNOWLEGMENTS

Holtec International generously allowed access to the FSAR for the HI-STORM 100 System, making possible construction of accurate and complete models of the system in place at the Hope Creek plant ISFSI. Special thanks are owed to the technical editor, Cornelia Brim, who provided efficient and timely assistance in the production of the final version of this document.

ACRONYMS AND ABBREVIATIONS

BWR	boiling water reactor
CFD	computational fluid dynamics
DOE	U.S. Department of Energy
DOE-NE	U. S. Department of Energy Office of Nuclear Energy
DSC	dry shielded canister
EPRI	Electric Power Research Institute
FEA	finite element analysis
ISFSI	independent spent fuel storage installation
MPC	multi-purpose canister
NCDC	National Climatic Data Center
NOAA	National Oceanic and Atmospheric Administration
ORNL	Oak Ridge National Laboratory
PNNL	Pacific Northwest National Laboratory

CONTENTS

FIGURES

TABLES

PRELIMINARY THERMAL MODELING OF HI-STORM 100S-218 VERSION B STORAGE MODULES AT HOPE CREEK NUCLEAR POWER STATION ISFSI

1.0 INTRODUCTION

As part of the Used Fuel Disposition Campaign of the U.S. Department of Energy, Office of Nuclear Energy (DOE-NE) Fuel Cycle Research and Development, a consortium of national laboratories[1] and industry[2] are performing visual inspections and temperature measurements of selected storage modules at various locations around the United States. In June 2012, inspections were performed on two horizontal storage modules in the Calvert Cliffs Nuclear Power Station's Independent Spent Fuel Storage Installation (ISFSI). Inspections are scheduled for late summer 2013 at the Hope Creek Nuclear Generating Station ISFSI, and for later in 2013 at the Diablo Canyon Power Plant ISFSI. Thermal analysis in support of these inspections is being undertaken at Pacific Northwest National Laboratory (PNNL). Pre-inspection and post-inspection evaluations for the modules inspected at Calvert Cliffs were performed using a detailed computational fluid dynamics (CFD) model of the storage module and the dry shielded canister (DSC) contained within it, using the STAR-CCM+ package. The results of these evaluations included temperature predictions in actual storage conditions for the module, DSC, and DSC contents, with preliminary estimates of fuel cladding temperatures (Suffield et al. 2012).

A similar effort is under way in support of the inspections at the Hope Creek Nuclear Generating Station ISFSI. This site utilizes the HI-STORM 100S-218 Version B vertical storage system developed by Holtec International. In this design, the spent fuel is sealed within a helium-pressurized stainless steel canister that is loaded into a vertical steel-lined concrete overpack. The thermal models are being developed using COBRA-SFS (Michener et al. 1995), a code developed by PNNL for thermal-hydraulic analysis of multi-assembly spent fuel storage and transportation systems. The COBRA-SFS code uses a finite-difference subchannel analysis approach for predicting flow and temperature distributions in spent fuel storage systems and fuel assemblies under forced and natural circulation flow conditions. It is applicable to both steady-state and transient conditions in single-phase gas-cooled spent fuel packages with radiation, convection, and conduction heat transfer. The code has been validated in blind pretest calculations using test data from spent fuel packages loaded with actual spent fuel assemblies as well as electrically heated single-assembly tests (Creer et al. 1987, Rector et al. 1986, Lombardo et al. 1986).

The data obtained in these on-site inspections provide an opportunity to develop structural and thermal models that can yield realistic predictions for actual storage systems, in contrast to

[1] Pacific Northwest National Laboratory, Oak Ridge National Laboratory, Sandia National Laboratories, and Idaho National Laboratory

[2] Electric Power Research Institute, TN/AREVA, Holtec International, PSEG Nuclear LLC (owner of Hope Creek Nuclear Generating Station), Constellation Energy (Owner of Calvert Cliffs Nuclear Power Station), and Pacific Gas and Electric Corporation (owner of Diablo Canyon Power Plant).

conservative and bounding design-basis calculations. The analytical approach used in this study does not include many of the conservatisms and bounding assumptions normally used in design-basis and safety-basis calculations for spent fuel storage systems.

The primary storage modules used for this study consist of four modules in the Hope Creek Nuclear Generating Station's ISFSI, designated as MPC-143, MPC-144, MPC-145, and MPC-146. Figure 1-1 shows an aerial view of the ISFSI, illustrating the layout of the double rows (2xN) of storage units. A typical HI-STORM100 module is illustrated in Figure 1-2. Development of the test plan for the inspection is ongoing, and the specific modules to be inspected will be determined based on the thermal analyses presented in this report, and the results of procedures testing on a system mock-up, to be performed by Holtec prior to the inspection. The four modules are essentially identical, except for the multi-purpose canister (MPC) contents, which vary somewhat in total decay heat load and loading pattern. Thermal evaluation models have been developed for all four modules, and calculational results are presented for all four modules, to have pre-inspection analyses for comparisons to data obtained from the module (or modules) actually inspected.

Figure 1-1. Aerial View of Hope Creek Nuclear Generating Station ISFSI, Showing Arrays of Vertical Storage Modules (Google 2011)

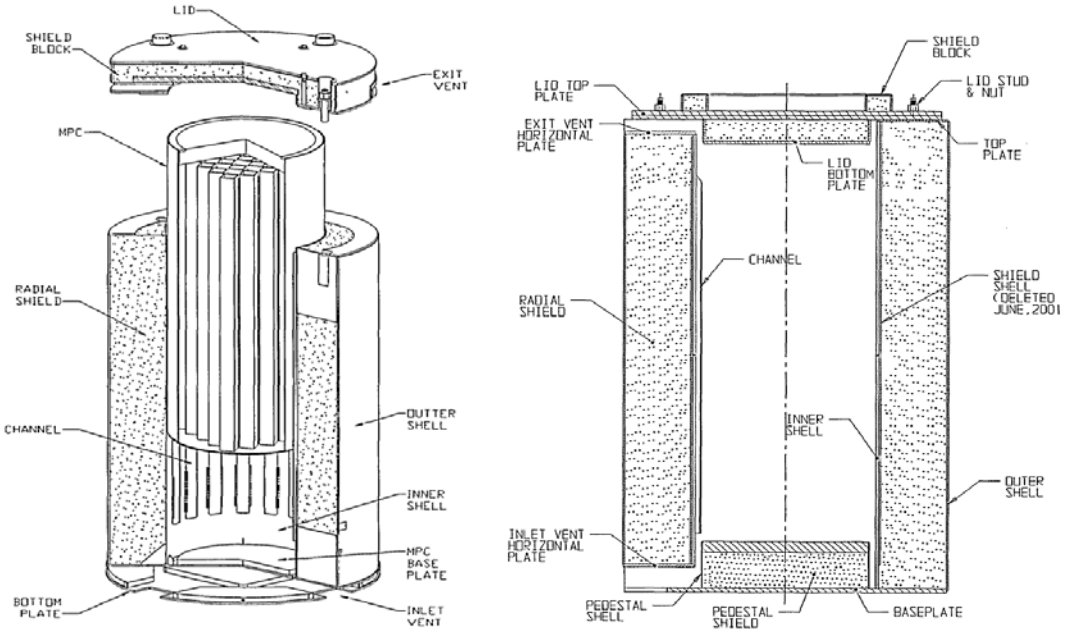

Figure 1-2. Typical HI-STORM 100 Vertical Storage Module (Image courtesy of Holtec International; reprinted with permission) NOTE: the 100S-218 Version B design used at Hope Creek differs in some details from this image.

The COBRA-SFS model geometry for the HI-STORM 100S-218 Version B with MPC-68 canister is described in detail in Section 2, along with the boundary conditions and modeling assumptions for the calculations to obtain predictions of long-term temperatures in the module(s) to be inspected. Section 3 presents pre-inspection predictions of component temperatures and temperature distributions within the module, based on the estimated decay heat loads in the MPCs as of the planned inspection timeframe of August 2013. A follow-on document will be issued post-inspection, which will include the pre-inspection results reported here as well as comparisons between pre-test predictions and inspection results, and further post-test calculations, if necessary, with appropriate discussion of results.

2.0 COBRA-SFS MODEL DESCRIPTION

The HI-STORM 100 system is a vertical storage module design developed by Holtec International, and consists of an MPC inserted into a steel-lined concrete overpack (Holtec 2010). The general design of the overpack is similar for all configurations of the system, such that the main site-specific character of a particular installation is the design of the canister stored within the overpack. At the Hope Creek ISFSI, the canister design is the MPC-68, which is for boiling water reactor (BWR) fuel, and stores up to 68 BWR fuel assemblies. The storage modules to be inspected in the Hope Creek ISFSI are designated MPC-143, MPC-144, MPC-145, and MPC-146. Each of these modules contains an MPC-68 canister. To avoid potential confusion with the MPC design designation used by Holtec and the module designation used at the Hope Creek ISFSI, the specific storage modules to be modeled in this evaluation are referred to as Module 143, Module 144, Module 145, and Module 146.

A COBRA-SFS model for a vertical storage system consists of three major pieces; the canister, the air flow channel that allows external ambient air to circulate through the module, and the external overpack surrounding the canister. The general structure of the model of the HI-STORM 100S-218 Version B storage system is illustrated in Figure 2-1. The detailed three-dimensional nodalization of the fuel assemblies, basket, canister, and overpack walls extends only over the axial length of the basket within the MPC. This highly detailed portion of the model represents the region of radial heat transfer from the fuel rods to the ambient environment. The axial length of this region is defined by the length of the basket, which in this case is only 5.24 cm (2.06 inches) short of the total axial length of the canister internal cavity. Axial heat transfer out the top and bottom of the system is represented with a simpler, one-dimensional thermal resistance network, consisting of the upper and lower plenum regions.

Diagrams illustrating the model representation of the entire system of Module 143 are shown in Figures 2-2 and 2-3. For clarity, the canister and overpack portions of the model are shown separately. Figure 2-2 shows a 3-D diagram of the canister portion of the model, including the fuel rods, fuel channel, basket plates (with neutron poison plates), basket support structure, and canister shell. Different colors are used for different components, for clarity in the complex mesh. This diagram is not to scale, since in a scaled diagram of the mesh, fine details such as the neutron poison plates and fuel channel are difficult to discern. In addition, the detailed rod-and-subchannel arrays within the fuel channel are shown with the rod spacing greatly exaggerated, so that the subchannels are visible.

Figure 2-3 shows a cross-section diagram of the portion of the model representing the overpack. The geometry of the other three modules is essentially identical to that of Module 143, and therefore the images in Figures 2-2 and 2-3 are applicable to the models for all four modules. The only significant difference in the models for the four modules is in the assembly loading pattern, which is unique for each module. The representation of the decay heat in the fuel assemblies in the COBRA-SFS model is discussed in detail in Section 2.1.

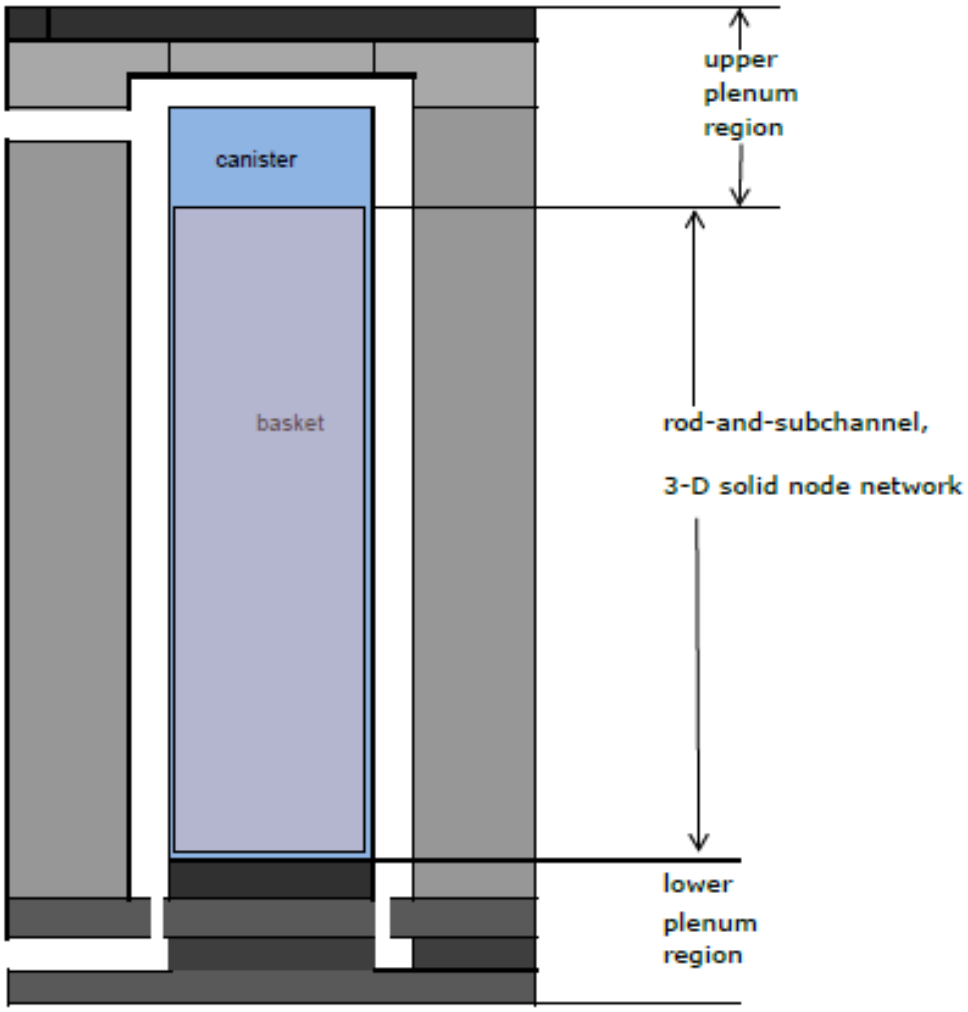

Figure 2-1. Diagram of Modeling Regions in COBRA-SFS Model of HI-STORM 100S-218 Version B Vertical Storage System (NOTE: diagram is not to scale)

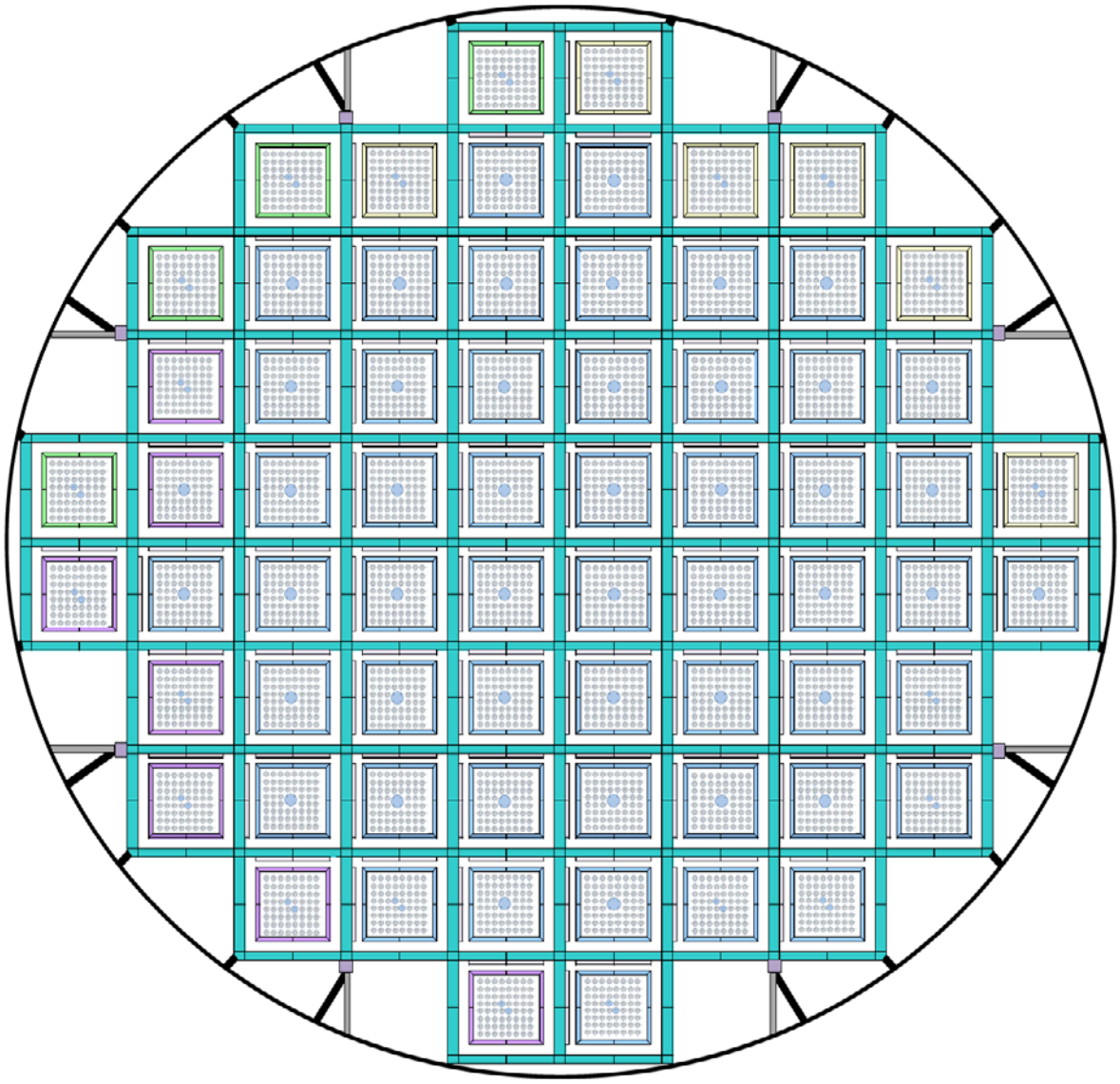

Figure 2-2. Diagram of 3-D COBRA-SFS Model of Canister for Module 143 (NOTE: diagram not to scale; node thicknesses greatly exaggerated for clarity)

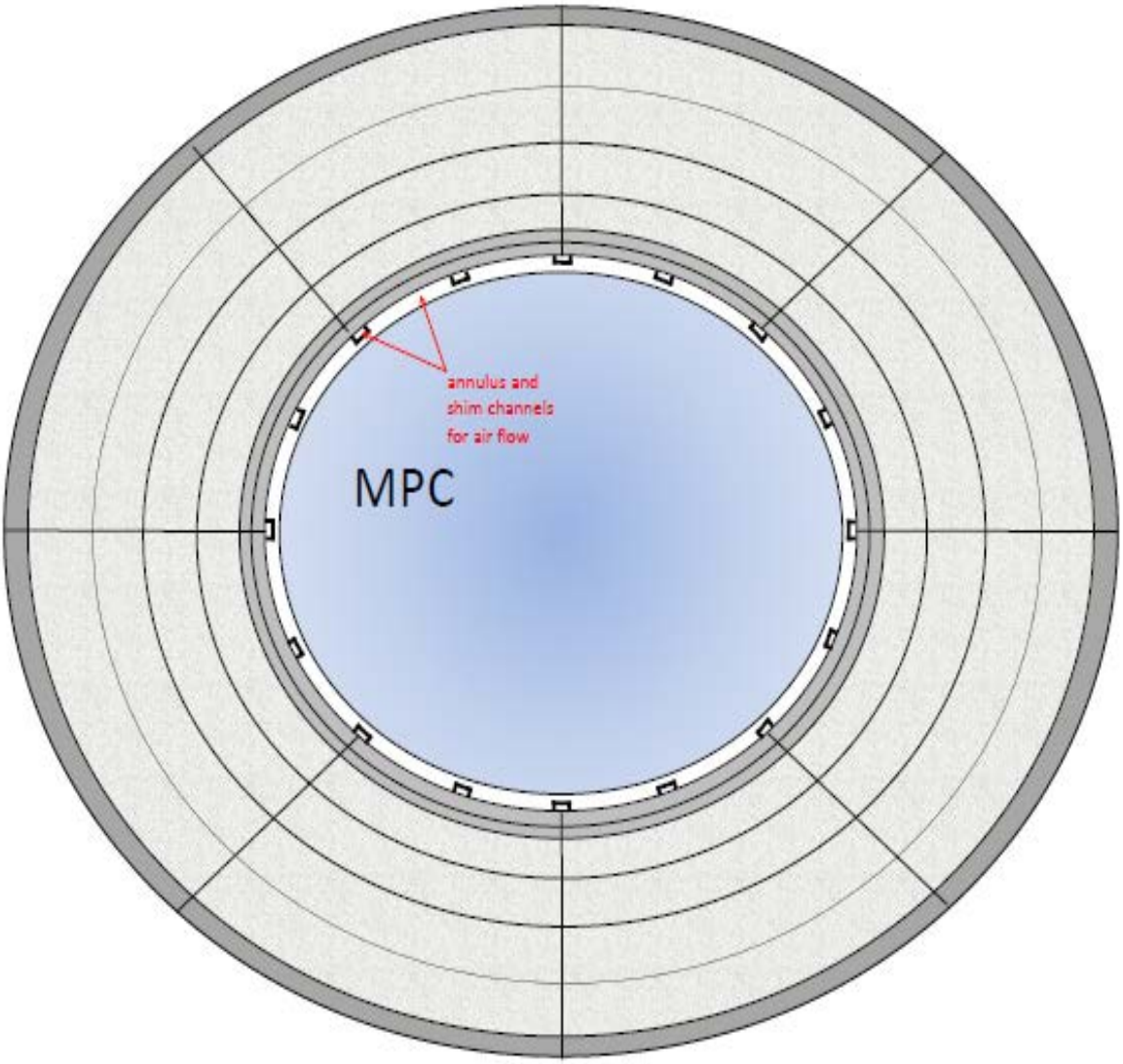

Figure 2-3. Cross-section of COBRA-SFS Model of Overpack for Module 143 (diagram is not to scale. Air annulus width and steel thicknesses are greatly exaggerated for clarity.)

The detailed model of the canister and internals (including the fuel assemblies) shown in Figure 2-2 has the typical mesh resolution generally used for the basket structure in COBRA-SFS models of spent fuel storage systems. Finer mesh resolution can be specified, if needed, but comparison with temperature measurements from single assembly and multi-assembly experiments, including testing of storage systems with spent fuel loaded in the basket (Lombardo et al. 1986; Rector et al. 1986; Creer et al. 1987) has shown that this meshing is sufficient for resolution of temperature gradients typical of spent fuel storage systems. The mesh includes the basket plates, poison plates, and basket support structures, including the shims on these structures that are used to ensure firm contact between the basket frame and canister inner shell.

The solid structure network also includes the thin plates of the zircaloy fuel channels containing the BWR fuel assemblies. The thermal network approach used in COBRA-SFS allows direct representation of thin plates and the contact resistance due to small gaps between adjacent components. In typical models for CFD and finite element analysis (FEA) codes, structures consisting of adjacent thin plates (such as the basket plates, poison plates, and poison plate sheathing) are modeled as a single material with homogenized properties that may include contact resistances. The approach used in COBRA-SFS modeling allows more detailed resolution of temperature distributions in such structures, using a comparatively smaller mesh.

As shown in Figure 2-2, the main feature of the COBRA-SFS model of the canister is the representation of the flow field within the fuel assemblies in the basket, and the flow paths external to the basket that allow recirculation due to natural convection within the canister. Within the individual basket cells, the fuel assembly and flow field are represented with a detailed subchannel model. This is illustrated in Figure 2-4 for a single assembly of each of the two different fuel configurations stored in the canisters at Hope Creek. This representation of the fuel assembly allows for much more accurate resolution of the local rod temperatures, compared to the typical approach used in CFD and FEA models, in which the fuel assembly region is represented as a homogeneous block with internal heat generation, or as a porous medium. The detailed rod and subchannel model allows the code to calculate individual fuel rod cladding temperatures, accounting for heat transfer by conduction, convection, and thermal radiation, and permits detailed modeling of material parameters, such as fuel cladding emissivity and surface conditions.

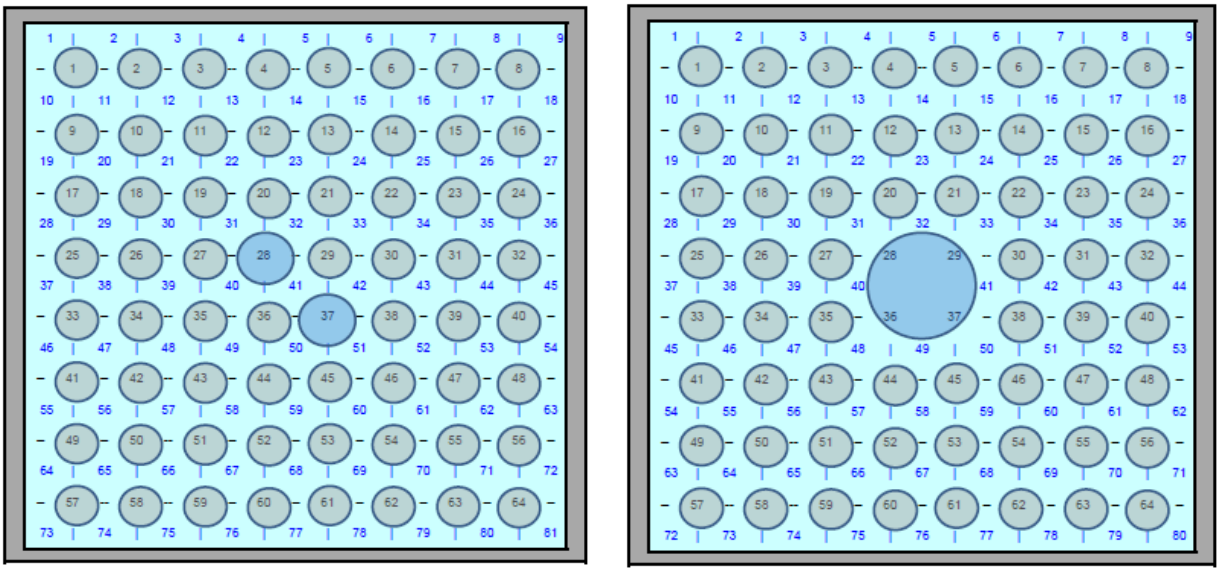

Figure 2-4. Rod-and-subchannel Array Diagram for COBRA-SFS Model of GE 8x8 Fuel Assemblies–GE7 and GE9 Configurations (Note: diagrams are not to scale; rod spacing is greatly exaggerated for clarity. Larger dark blue circles represent water rods.)

For convection heat transfer, the fluid channels within the canister are thermally connected to the fuel rods and to the surrounding solid conduction nodes representing the basket by means of a user-specified heat transfer correlation. Based on validation of the COBRA-SFS code with

experimental data from vertical test systems and canisters loaded with actual spent fuel, convection heat transfer in the fuel rod array is represented with the venerable Dittus-Boelter heat transfer correlation for turbulent flow,

$$Nu = 0.023(Re^{0.8})(Pr^{0.4})$$

where Nu = Nusselt number
Re = Reynolds number, based on subchannel hydraulic diameter
Pr = Prandtl number for the backfill gas

For laminar flow conditions, a Nusselt number of 3.66 has been verified as applicable to spent fuel rod arrays. The local heat transfer coefficient is defined as the minimum of the values calculated from the laminar and turbulent correlations specified by user input. Figure 2-5 illustrates the convenient mathematical behavior of these correlations as a function of Reynolds number.

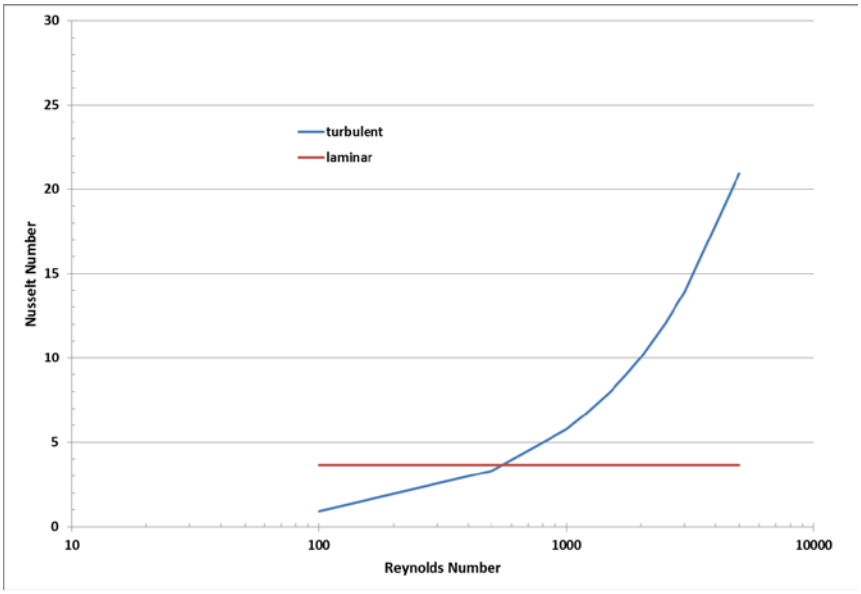

Figure 2-5. Laminar and Turbulent Formulations for Nusselt Number

In addition to convection heat transfer, the fluid energy equation includes conduction through the fluid (helium gas) in the subchannels, and the gas is assumed transparent to thermal radiation. Thermal radiation within the basket is calculated using 2-dimensional (planar cross-section) grey-body view factors for the rod array and surrounding solid conduction nodes of the basket wall. The view factors are calculated for the specific assembly and basket cell geometry using the auxiliary code RADGEN, which is part of the COBRA-SFS package. Thermal radiation across the geometrically simpler flow channels between the basket and the canister shell are determined from user-input black body view factors, calculated using the Hottel crossed-string correlation methodology. Based on the specified surface emissivity of the nodes of the surfaces of a given flow region, the code calculates the grey-body view factors for thermal radiation exchange.

The annulus between the canister and the overpack is represented in the COBRA-SFS model with 20 flow channels to represent the circumferential variation in the annulus region cross-section due to the 16 shim channels spaced around the inner shell of the storage cavity (see Figure 2-3). The shim channels are open at top and bottom, and therefore constitute isolated flow paths for air circulation within the annulus. These flow paths are treated as separate parallel channels in the COBRA-SFS model. Air flow in the fluid channels representing the annulus is calculated using a pressure drop boundary condition based on the height of system and the specified ambient air temperature. Momentum losses are determined using a friction factor correlation and form drag losses due to the orificing effects of the inlet and exit structures above and below the annulus.

Thermal connections between the annulus flow channels and the solid conduction nodes of the MPC shell, shim channel structures, and overpack inner shell are defined in the COBRA-SFS model for conduction and thermal radiation heat transfer. Convection heat transfer in the air annulus is treated as a forced convection flow, driven by the imbalance between the hydrostatic pressure drop within the annulus and that of the ambient air external to the overpack (Sparrow and Azevedo 1985). The Dittus-Boelter correlation has been shown to be an appropriate heat transfer model for prediction of heat transfer in a vertical storage module (Creer et al., 1987), but requires two minor modifications for application to the specific annulus geometry of the HI-STORM 100 system. The definition of the annulus hydraulic diameter used in the heat transfer correlation's database is twice the radial width of the annulus (i.e., 2*W). The channel hydraulic diameter is defined in COBRA-SFS using the more general formula of four times the flow area divided by the wetted perimeter.

These two formulations are exactly equivalent for a simple circular annulus, but the annulus in the HI-STORM 100 system contains 16 channel shims, to center the MPC within the overpack cavity (as illustrated in the diagram in Figure 2-3.) The presence of the shims effectively reduces the hydraulic diameter by approximately 50%, when calculated using the more general formula. However, evaluations by Holtec have validated appropriate agreement with heat transfer data in a vertical storage module (from Creer et al. 1987) using the Dittus-Boelter correlation for heat transfer in the annulus, with the hydraulic diameter defined as 2*W and the Prandtl number coefficient[3] specified as 0.333.

The equivalent formulation of this variation on the Dittus-Boelter correlation for COBRA-SFS is obtained by specifying the Nusselt number for turbulent flow heat transfer in the annulus channels as

$$Nu = 0.046\ Re^{0.8}Pr^{0.33}$$

where Re = Reynolds number, based on flow channel hydraulic diameter
Pr = Prandtl number for air

[3] The Dittus-Boelter correlation is derived with the general formulation $Nu = C\ Re^{m}Pr^{n}$, where C=0.023, m=0.8, and specifies n=0.4 for heating and n=0.3 for cooling. The original database did not investigate the effects of heating on one wall and cooling on the other, as is the situation in the HI-STORM 100 annulus.

The air flow in the annulus is expected to be turbulent for normal conditions of storage, but the COBRA-SFS input also includes a lower bound of Nu = 7.44 (derived[4] from Sparrow et al., 1961), which represents laminar flow conditions in a vertical stack. As illustrated in Figure 2-5, the code uses the mathematical behavior of the correlations to automatically select the appropriate flow regime by taking the maximum of the values obtained with the laminar and turbulent formulations for the local flow conditions.

2.1 Fuel Assembly Decay Heat Modeling

The spent fuel stored at Hope Creek consists of GE 8x8 assemblies in two main configurations, designated GE7 and GE9, as noted above in the discussion of fuel assembly geometry modeling with COBRA-SFS. The GE7 configuration has nominally 62 active fuel rods, with two water rods near the center of the array. The GE9 configuration has nominally 60 active fuel rods, with a large central water rod that displaces four rod positions in the array. Information transmitted from PSEG Nuclear Fuels[5] provided the total canister decay heat loads, calculated assembly decay heat loads, and assembly load maps for the canisters in all four of the modules being considered for inspection. The package included individual assembly decay heat values calculated with ORIGEN[6] and with a second methodology[7] based on Regulatory Guide 3.54 (NRC 1999).

The total canister decay heat loadings for the four Modules are summarized in Table 2-1. This table includes the values reported for the time of loading and for the scheduled time of the inspection, as calculated with the two methodologies. The design basis maximum thermal loading for the MPC-68 in above-ground HI-STORM 100 storage systems is 0.5 kW per assembly, for a total decay heat load of 34 kW. The decay heat at the time of loading of these canisters was therefore 37% of design basis, based on the ORIGEN modeling. Based on the more conservative RG 3.54 modeling, the initial decay heat load was 47% of design basis.

Table 2-1. Total Decay Heat Loading per Module

	ORIGEN			**RG 3.54**	
	decay heat (kW)			**decay heat (kW)**	
	at loading	**at inspection**		**at loading**	**at inspection**
Module	**(11/2006)**	**(8/2013)**		**(11/2006)**	**(8/2013)**
143	12.69	10.44		16.01	12.78
144	12.02	9.29		16.03	11.40
145	10.71	9.24		12.89	11.13
146	10.84	9.33		13.03	11.25

[4] The mean value in the reference is Nu=7.86. The value of 7.44 represents the lower bound on the ±5% uncertainty in the data.

[5] Provided in **Transmittal of Design Information**, NF ID# NFS 13-060; *Data for Fuel Loaded into Hope Creek MPC143, MPC144, MPC145 and MPC146*, non-safety related, verified information. Approved 6/3/2013.

[6] The specific version of ORIGEN used is identified in an e-mail from Steven P. Baker of PSEG Nuclear Fuels (sent 7/25/2013 7:09am PDT) as ORIGEN-ARP packaged with SCALE 6.1.1. A current reference for ORIGEN-ARP is ORNL/TM-2005/39, *ORIGEN-ARP: Automatic Rapid Processing for Spent Fuel Depletion, Decay, and Source Term Analysis*. Oak Ridge National Laboratory, Oak Ridge, Tennessee, 2009.

[7] Regulatory Guide 3.54 endorses methodology documented in NUREG/CR-5625, **Technical Support for a Proposed Decay Heat Guide Using SAS2H/ORIGEN-S Data**, OW Hermann, CV Parks, and JP Renier, Oak Ridge National Laboratory, Oak Ridge, Tennessee. July 1994.

The RG 3.54 methodology produces decay heat values that are on average 22% higher than the values obtained with the ORIGEN methodology. The total decay heat load among the four Modules varies by about 13% with the ORIGEN results, and by about 15% with the RG 3.54 results. The decay heat values for all assemblies within the individual canisters are listed in Table 2-2. This table includes both the ORIGEN results and the RG 3.54 results for each assembly. The basket location of an assembly is identified by row number and column letter, as illustrated with the diagram in Figure 2-6.

Table 2-2. Projected Assembly Decay Heat Loading as of August 2013 for Each Module

Basket cell location	Assembly decay heat (kW) ORIGEN					Assembly decay heat (kW) RG 3.54			
	Module 143	Module 144	Module 145	Module 146		Module 143	Module 144	Module 145	Module 146
E-1	0.1045	0.0323	0.1012	0.1031		0.1248	0.0357	0.1187	0.1211
F-1	0.1038	0.0328	0.0981	0.1023		0.1227	0.0362	0.1164	0.1200
C-2	0.0978	0.0327	0.1010	0.1022		0.1160	0.0362	0.1185	0.1199
D-2	0.1061	0.1192	0.1010	0.1018		0.1262	0.1425	0.1184	0.1194
E-2	0.1753	0.1608	0.1528	0.1614		0.2151	0.1945	0.1853	0.1954
F-2	0.1713	0.1842	0.1579	0.1548		0.2163	0.2274	0.1915	0.1896
G-2	0.1026	0.1194	0.1010	0.1030		0.1215	0.1426	0.1184	0.1211
H-2	0.1073	0.0330	0.1017	0.1011		0.1284	0.0364	0.1194	0.1185
B-3	0.1030	0.0322	0.1009	0.1021		0.1210	0.0355	0.1184	0.1198
C-3	0.1562	0.1846	0.1564	0.1585		0.1960	0.2281	0.1893	0.1943
D-3	0.1774	0.1581	0.1538	0.1582		0.2226	0.1918	0.1870	0.1917
E-3	0.1735	0.1963	0.1529	0.1630		0.2122	0.2455	0.1854	0.1990
F-3	0.1770	0.1962	0.1565	0.1541		0.2150	0.2456	0.1896	0.1864
G-3	0.1781	0.1417	0.1564	0.1564		0.2193	0.1693	0.1894	0.1894
H-3	0.1771	0.1782	0.1583	0.1590		0.2230	0.2194	0.1923	0.1950
J-3	0.1009	0.0323	0.1009	0.1024		0.1184	0.0357	0.1184	0.1202
B-4	0.1072	0.1192	0.1009	0.1023		0.1283	0.1425	0.1183	0.1201
C-4	0.1782	0.1429	0.1580	0.1584		0.2156	0.1722	0.1909	0.1923
D-4	0.1670	0.1964	0.1547	0.1525		0.2043	0.2464	0.1895	0.1850
E-4	0.1908	0.1965	0.1532	0.1536		0.2350	0.2458	0.1848	0.1867
F-4	0.1743	0.1952	0.1543	0.1552		0.2119	0.2445	0.1866	0.1893
G-4	0.1698	0.1945	0.1516	0.1564		0.2076	0.2450	0.1834	0.1893
H-4	0.1739	0.1352	0.1567	0.1578		0.2127	0.1624	0.1894	0.1930
J-4	0.1030	0.1172	0.1011	0.1025		0.1228	0.1367	0.1185	0.1213
A-5	0.1029	0.0328	0.1014	0.0978		0.1227	0.0362	0.1189	0.1160
B-5	0.1787	0.1461	0.1575	0.1600		0.2179	0.1755	0.1927	0.1959
C-5	0.1892	0.1964	0.1508	0.1544		0.2449	0.2459	0.1817	0.1867
D-5	0.1605	0.1955	0.1577	0.1561		0.1963	0.2465	0.1921	0.1887
E-5	0.1592	0.1962	0.1584	0.1443		0.1952	0.2455	0.1934	0.1778
F-5	0.1676	0.1955	0.1561	0.1565		0.2051	0.2465	0.1886	0.1895
G-5	0.1928	0.1945	0.1443	0.1616		0.2373	0.2450	0.1779	0.1971
H-5	0.1810	0.1956	0.1550	0.1538		0.2271	0.2466	0.1891	0.1871
J-5	0.1928	0.1354	0.1568	0.1614		0.2430	0.1630	0.1894	0.1969
K-5	0.1069	0.0111	0.1011	0.0981		0.1264	0.0120	0.1185	0.1163
A-6	0.0983	0.0328	0.1021	0.1032		0.1166	0.0362	0.1198	0.1212

Basket cell location	Assembly decay heat (kW) ORIGEN					Assembly decay heat (kW) RG 3.54			
	Module 143	Module 144	Module 145	Module 146		Module 143	Module 144	Module 145	Module 146
B-6	0.1957	0.1698	0.1548	0.1529		0.2465	0.2078	0.1896	0.1854
C-6	0.1785	0.1964	0.1574	0.1541		0.2174	0.2466	0.1920	0.1863
D-6	0.1904	0.1966	0.1558	0.1525		0.2344	0.2460	0.1907	0.1851
E-6	0.1922	0.1952	0.1540	0.1563		0.2345	0.2444	0.1905	0.1889
F-6	0.1919	0.1951	0.1508	0.1612		0.2350	0.2444	0.1826	0.1966
G-6	0.1930	0.1946	0.1582	0.1551		0.2374	0.2451	0.1917	0.1892
H-6	0.1757	0.1963	0.1549	0.1541		0.2139	0.2455	0.1896	0.1863
J-6	0.1958	0.1826	0.1506	0.1629		0.2472	0.2253	0.1824	0.1989
K-6	0.1017	0.0328	0.1011	0.1031		0.1194	0.0362	0.1186	0.1211
B-7	0.1077	0.1189	0.1011	0.1032		0.1292	0.1423	0.1186	0.1212
C-7	0.1826	0.1775	0.1553	0.1581		0.2253	0.2183	0.1894	0.1910
D-7	0.1786	0.1952	0.1562	0.1512		0.2178	0.2445	0.1887	0.1830
E-7	0.1864	0.1965	0.1540	0.1616		0.2273	0.2459	0.1906	0.1957
F-7	0.1772	0.1955	0.1565	0.1541		0.2158	0.2466	0.1895	0.1907
G-7	0.1763	0.1946	0.1551	0.1544		0.2148	0.2450	0.1893	0.1867
H-7	0.1845	0.1367	0.1574	0.1631		0.2321	0.1642	0.1918	0.1991
J-7	0.1062	0.1190	0.1012	0.1011		0.1255	0.1424	0.1187	0.1185
B-8	0.1010	0.0306	0.0981	0.1010		0.1185	0.0337	0.1164	0.1185
C-8	0.1699	0.1485	0.1543	0.1557		0.2080	0.1797	0.1866	0.1905
D-8	0.1783	0.1535	0.1509	0.1509		0.2196	0.1852	0.1818	0.1817
E-8	0.1820	0.1964	0.1569	0.1509		0.2302	0.2466	0.1898	0.1817
F-8	0.1824	0.1965	0.1534	0.1601		0.2250	0.2466	0.1852	0.1960
G-8	0.1906	0.1823	0.1582	0.1532		0.2412	0.2251	0.1920	0.1849
H-8	0.1774	0.1543	0.1576	0.1569		0.2182	0.1867	0.1928	0.1898
J-8	0.1083	0.0252	0.1010	0.1030		0.1298	0.0281	0.1184	0.1210
C-9	0.1070	0.0307	0.1011	0.1032		0.1281	0.0338	0.1185	0.1212
D-9	0.1060	0.1190	0.1010	0.1026		0.1261	0.1424	0.1184	0.1215
E-9	0.1976	0.1443	0.1569	0.1583		0.2436	0.1778	0.1899	0.1920
F-9	0.2019	0.1363	0.1538	0.1600		0.2496	0.1638	0.1871	0.1959
G-9	0.1062	0.1194	0.1011	0.1027		0.1255	0.1426	0.1186	0.1215
H-9	0.1021	0.0281	0.0979	0.1023		0.1199	0.0311	0.1161	0.1201
E-10	0.1023	0.0329	0.1009	0.1021		0.1201	0.0363	0.1184	0.1199
F-10	0.1076	0.0322	0.0978	0.1022		0.1291	0.0355	0.1160	0.1199

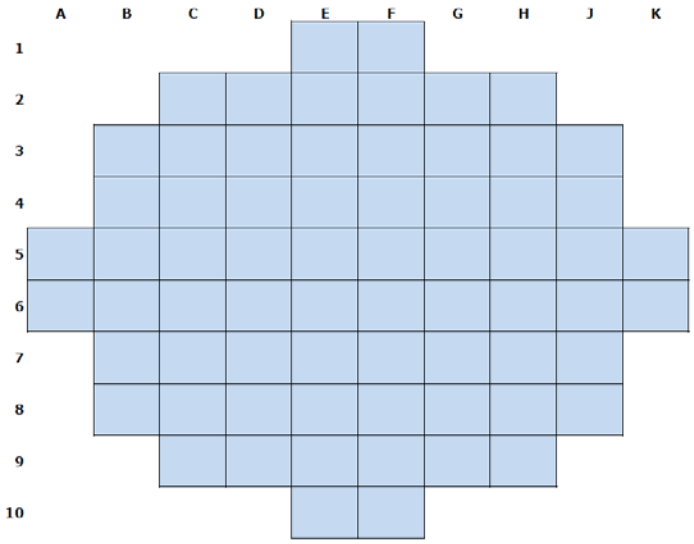

Figure 2-6. Diagram Illustrating Basket Cell Location Convention

The axial decay heat profile assumed for the GE 8x8 fuel within the canisters was modeled with a generic profile for BWR fuel, since axial burnup distributions for the fuel were not included in the fuel data package from Hope Creek. This profile, shown in Figure 2-7, is based on representative burnup distributions for BWR fuel (Turner 1989). More accurate information on the axial decay heat profile would result in more accurate predictions of peak component temperatures within the canister. Because the profile for spent fuel is relatively flat, the uncertainty in peak temperature predictions due to this approximation is probably rather small. Near the ends of the fuel region, however, the profile is expected to drop to near zero over a relatively short distance. This gradient strongly influences the temperature profile near the ends of the canister. The generic profile, rather than profiles representative of the fuel stored in these modules, is a potential source of uncertainty in the predictions of axial temperature distribution in the thermal modeling.

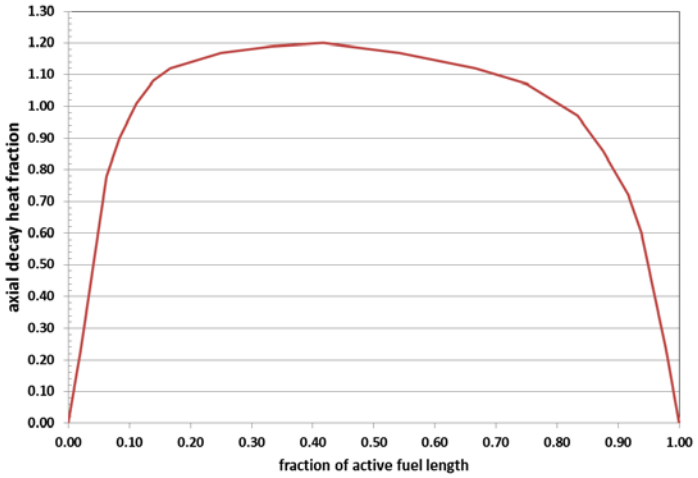

Figure 2-7. Generic Axial Decay Heat Profile for BWR Spent Fuel

2.2 Ambient Conditions

Ambient conditions at the time of the inspection are expected to have a significant effect on the temperatures that will be measured in the storage module. The inspection plans include inserting a specially designed thermal probe down into the annulus, and obtaining outer shell surface temperature measurements along the axial length of the canister. Because the primary mode of heat removal from the canister at the outer shell is convection to the air flowing up the annulus, the shell surface temperature is directly dependent on the inlet air temperature.

For the pre-inspection evaluations, since it is not known what the air temperature will be at the time of the inspection, an average ambient temperature of 80°F (27°C) was assumed in these calculations. This happens to be the design basis ambient air temperature for the HI-STORM 100 systems. It is also a reasonable estimate of typical average daytime ambient temperatures at the Hope Creek ISFSI site in high summer, based on data[8] obtained from the National Oceanic and Atmospheric Administration (NOAA 2013). This is illustrated by the plot in Figure 2-8, showing monthly maximum, minimum, and average temperatures over the past year, from August 2012 to July 2013. Figure 2-9 shows the average maximum and average minimum temperatures on a monthly basis over this time period.

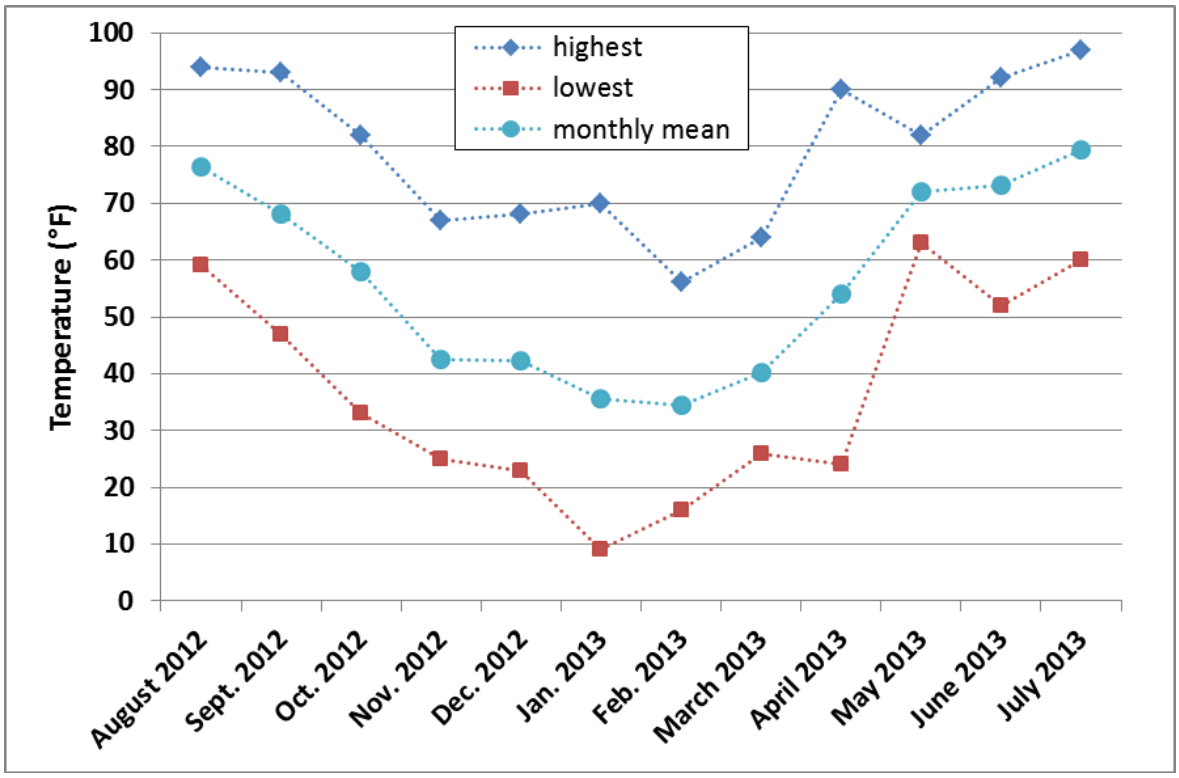

Figure 2-8. Monthly Maximum, Minimum, and Average Temperatures Reported at the New Castle County Airport, Wilmington, Delaware (NOAA 2013)

[8] This data will be archived after final quality control review (after the end of 2013), by the National Climatic Data Center (NCDC), and will be publicly available at http://www.ncdc.noaa.gov.

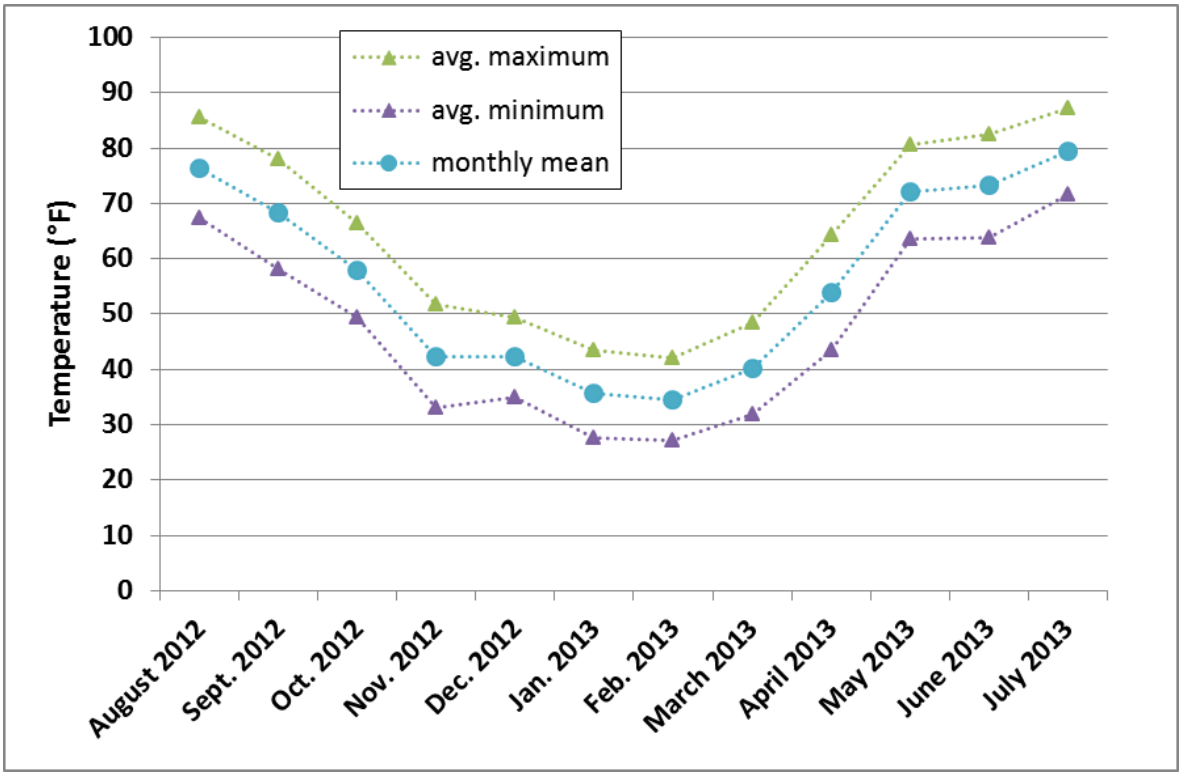

Figure 2-9. Monthly Average Maximum and Minimum Temperatures Reported at the New Castle County Airport, Wilmington, Delaware (NOAA 2013)

The temperature data shown in Figures 2-8 and 2-9 are archived data from the reporting station at the New Castle County Airport in Wilmington, Delaware, approximately 18 miles northeast of the Hope Creek plant. This station is the NOAA weather reporting station for the surrounding area, including Hancocks Bridge, New Jersey, where the plant is located. Ambient temperature data from a monitoring station located at the ISFSI would yield a more accurate estimate of local ambient conditions, but such data is not available.

Because of the uncertainty in local ambient conditions and the shifting time-frame of the inspection, an additional set of calculations were performed over a range of assumed ambient conditions. These calculations were performed only for Modules 144 and 145, which have been identified[9] as the specific modules that will be inspected. The range of ambient conditions evaluated are for an extraordinarily hot day at 90°F (32.2°C) and a more moderate day at 70°F (21.1°C). In addition, because there is a possibility that the inspection may not be performed until late autumn, a third case assumed a chilly ambient of 50°F (10°C).

In all cases, these ambient conditions assume still air. Consideration of wind effects in the current modeling effort would require detailed information on wind speed, direction, and variation over time at the ISFSI location, to estimate the effect on flow velocities at the inlet vents of the specific modules to be inspected. By definition, this information is not available for

[9] Marschman, S. 2013. Email message from Steve Marschman (Idaho National Laboratory to Harold E. Adkins (of PNNL) "More", sent Monday, August 12, 2013 10:20am (PDT).

pre-inspection calculations. The study of wind effects on storage system performance is a topic of some interest in general for a number of reasons, but it is beyond the scope of the current work.

The external solar heat load on the modules assumed for these calculations is based on the solar radiation assumptions specified in 10 CFR 71.71 (10 CFR 71). This regulation is specifically for transport conditions, but the specified values are generally used for stationary storage systems, as well. Solar radiation over a 12-hour period is defined in 10 CFR 71.71 as

- 800 cal/cm^2 (2950 Btu/ft^2) for horizontal surfaces
- 400 cal/cm^2 (1475 Btu/ft^2) for curved surfaces.

Adjusting for the surface emissivity, which in these evaluations is assumed to be 0.9 for the painted exterior surfaces of the overpack, the above specified values are averaged over a 24-hour period, to obtain the following solar heat flux values for this system:

- 349 W/m^2 (110.6 Btu/hr-ft^2) on the overpack lid
- 175 W/m^2 (55.3 Btu/hr-ft^2) on the outer shell.

These values may be conservative for the solar heat load on the modules at the time of the actual inspection, but in the absence of site-specific information, they will have to do.

3.0 PRE-INSPECTION PREDICTIONS OF COMPONENT TEMPERATURES

The COBRA-SFS model described in Section 2 was used to obtain predictions of component temperatures within the four modules being considered for inspection at the Hope Creek ISFSI. (As of mid-August 2013, Modules 144 and 145 have been selected as the modules to be inspected.) Calculations were performed for the total decay heat values and assembly decay heat distributions provided based on the ORIGEN methodology and the RG 3.54 methodology. These calculations assume an average ambient temperature of 80°F (27°C), in still air, with external solar heat load as specified in 10 CFR 71. Table 3-1 summarizes peak temperatures predicted for components of the canister for each case. Table 3-2 summarizes peak temperatures predicted for components of the overpack.

Table 3-1. Peak Component Temperatures, °F (°C), in MPCs (ambient 80°F (27°C))

	Fuel cladding	**Fuel channel**	**Basket plate**	**Basket periphery**	**Basket support**	**Canister inner surface**	**Canister outer surface**
ORIGEN							
Module 143	264 (128.7)	262 (127.5)	262 (127.5)	214 (101.0)	200 (93.4)	170 (76.9)	169 (76.1)
Module 144	254 (123.2)	252 (122.2)	252 (122.2)	209 (98.2)	194 (90.0)	165 (74.1)	164 (73.4)
Module 145	244 (117.5)	242 (116.7)	242 (116.7)	200 (93.4)	188 (86.7)	162 (72.3)	161 (71.6)
Module 146	245 (118.2)	243 (117.3)	243 (117.3)	201 (93.8)	189 (87.2)	163 (72.6)	161 (71.9)
RG 3.54							
Module 143	296 (146.6)	294 (145.3)	294 (145.3)	238 (114.2)	221 (105.2)	185 (85.2)	184 (84.2)
Module 144	285 (140.7)	283 (139.6)	283 (139.6)	232 (111.3)	215 (101.5)	180 (82.1)	178 (81.2)
Module 145	270 (132.1)	268 (131.2)	268 (131.2)	220 (104.2)	206 (96.4)	174 (79.1)	173 (78.3)
Module 146	271 (133.0)	269 (131.9)	269 (131.9)	221 (104.8)	207 (97.0)	175 (79.5)	174 (78.6)

Table 3-2. Peak Component Temperatures, °F (°C), in Overpack (ambient 80°F (27°C))

	Annulus shims	**Overpack inner shell**	**Overpack concrete**	**Overpack outer shell**	**Overpack lid inner surface**	**Overpack lid outer surface**
ORIGEN						
Module 143	169 (76.1)	169 (75.9)	165 (73.6)	94 (34.3)	110 (43.3)	96 (35.3)
Module 144	164 (73.4)	163 (73.2)	164 (73.2)	94 (34.2)	109 (42.7)	95 (35.2)
Module 145	161 (71.4)	160 (71.4)	157 (69.4)	93 (34.1)	108 (42.2)	95 (35.2)
Module 146	161 (71.7)	161 (71.7)	157 (69.6)	93 (34.1)	108 (42.3)	95 (35.2)
RG 3.54						
Module 143	183 (84.0)	183 (84.0)	178 (81.3)	95 (34.8)	113 (45.3)	96 (35.5)
Module 144	178 (81.0)	178 (80.9)	173 (78.4)	94 (34.6)	112 (44.6)	96 (35.5)
Module 145	173 (78.1)	172 (78.0)	168 (75.6)	94 (34.4)	111 (43.8)	96 35.4
Module 146	173 (78.4)	173 (78.4)	169 (76.0)	94 (34.4)	111 (43.9)	96 35.4

Axial temperature distributions on the canister shell are presented in Figures 3-1 through 3-4 for the four modules. These plots show temperatures determined for the decay heat values from the ORIGEN methodology and from the RG 3.54 methodology. The RG 3.54 methodology yields somewhat higher temperatures, due to the higher decay heat values predicted for the fuel within the modules. For a given methodology, however, the axial temperature profiles on the canister shell are very similar.

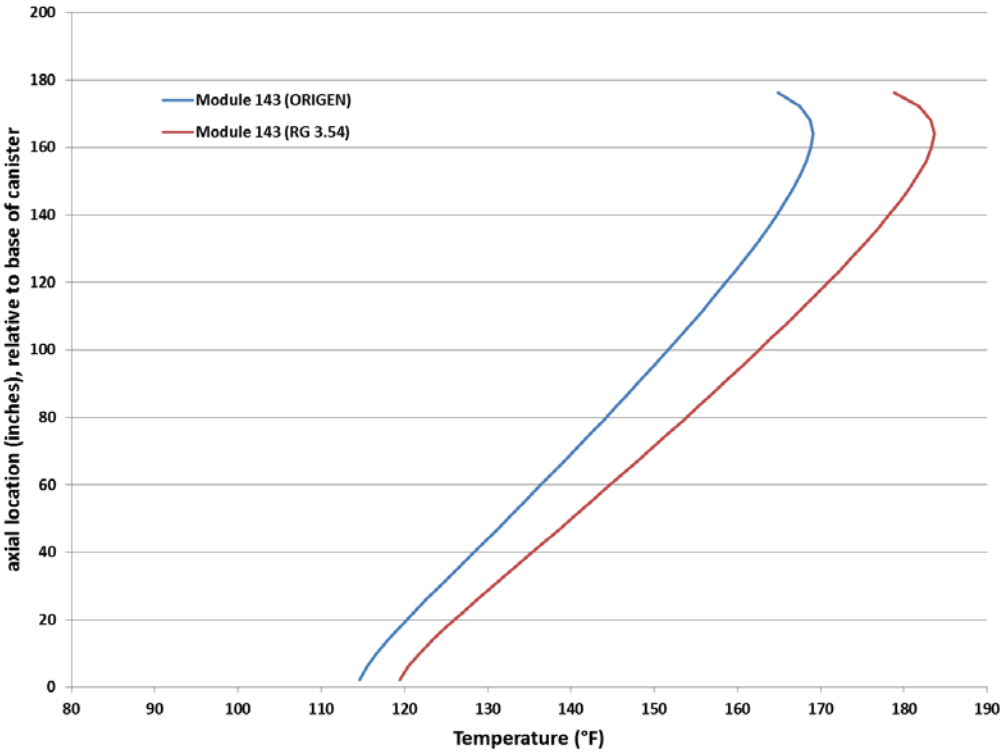

Figure 3-1. Axial Temperature Profile on MPC Outer Shell: Module 143 (80°F (27°C) ambient

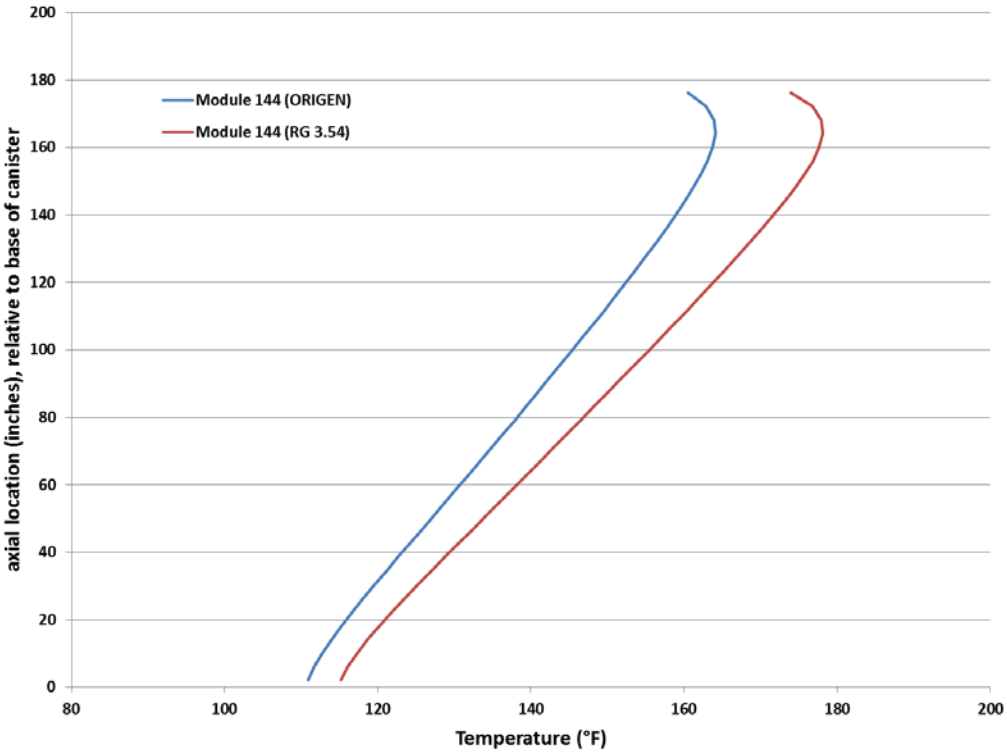

Figure 3-2. Axial Temperature Profile on MPC Outer Shell: Module 144 (80°F (27°C) ambient

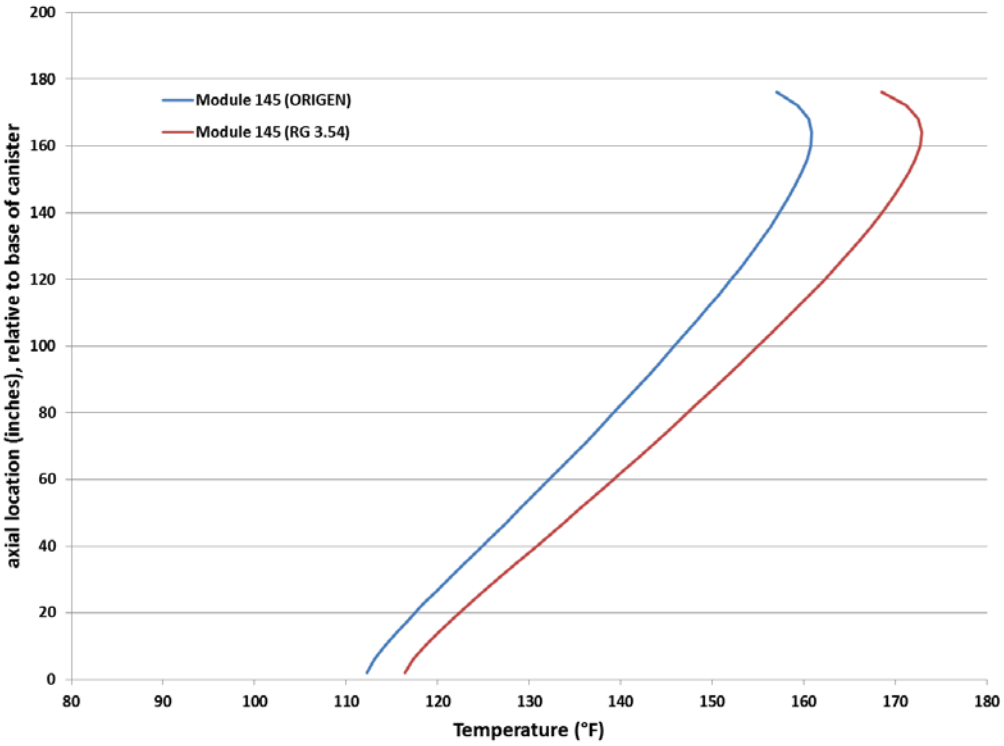

Figure 3-3. Axial Temperature Profile on MPC Outer Shell: Module 145 (80°F (27°C) ambient

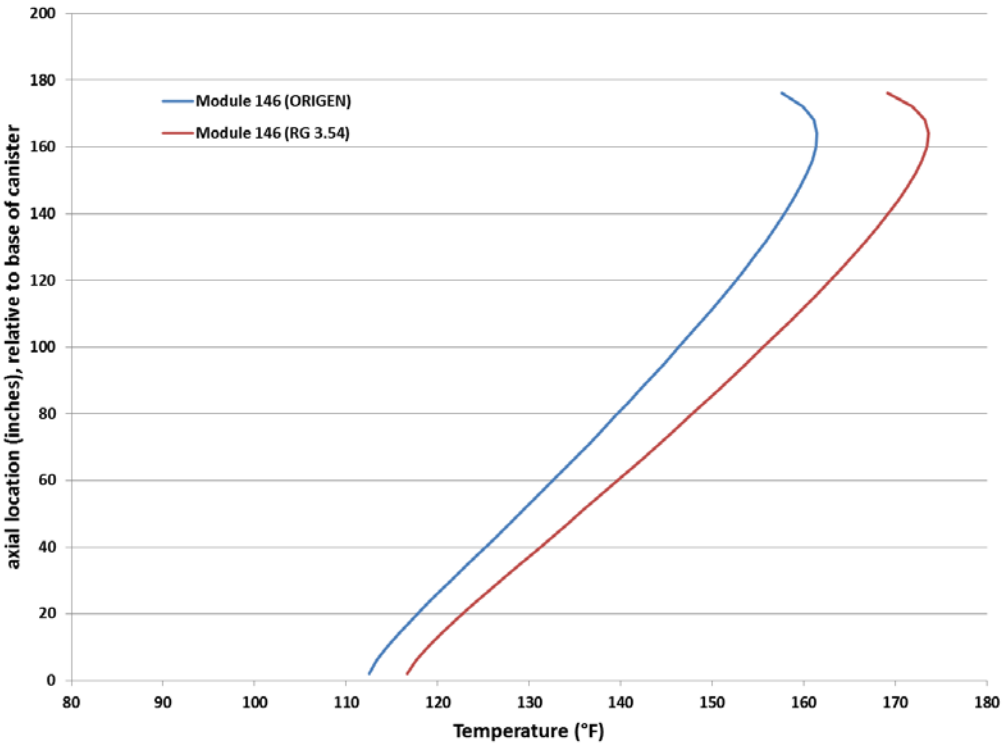

Figure 3-4. Axial Temperature Profile on MPC Outer Shell: Module 146 (80°F (27°C) ambient

The axial temperature profiles shown in Figures 3-1 through 3-4 are on a vertical line through the peak canister shell temperature location. However, the circumferential variation in predicted temperature at any given axial location on the canister shell is quite small. The symmetrical geometry of the air flow path through the module (i.e., inlet vents, annulus, and outlet vents), is designed to assure uniform distribution of air around the annulus between the canister shell and the overpack inner wall. In the 100S Version B design specifically, the air inlet flow path through the upper base plate provides an extremely effective flow distributor to ensure uniform distribution of air flow into the annulus.

Given the geometric design of the system and the assumption of still air external to the module, the only significant source of circumferential variation in predicted temperatures is in asymmetries in the fuel loading pattern within the canister basket. However, close examination of the loading patterns within the baskets of these four canisters (refer to Table 2-2) shows that the distribution of the decay heat load in each individual canister is remarkably symmetrical. This is illustrated in Figure 3-5, with plots of the decay heat values (from ORIGEN) in the peripheral assemblies of the basket (refer to Figure 2-6 for basket cell numbering convention.) Table 3-3 summarizes the maximum, minimum, and average assembly decay heat values for these peripheral assemblies.

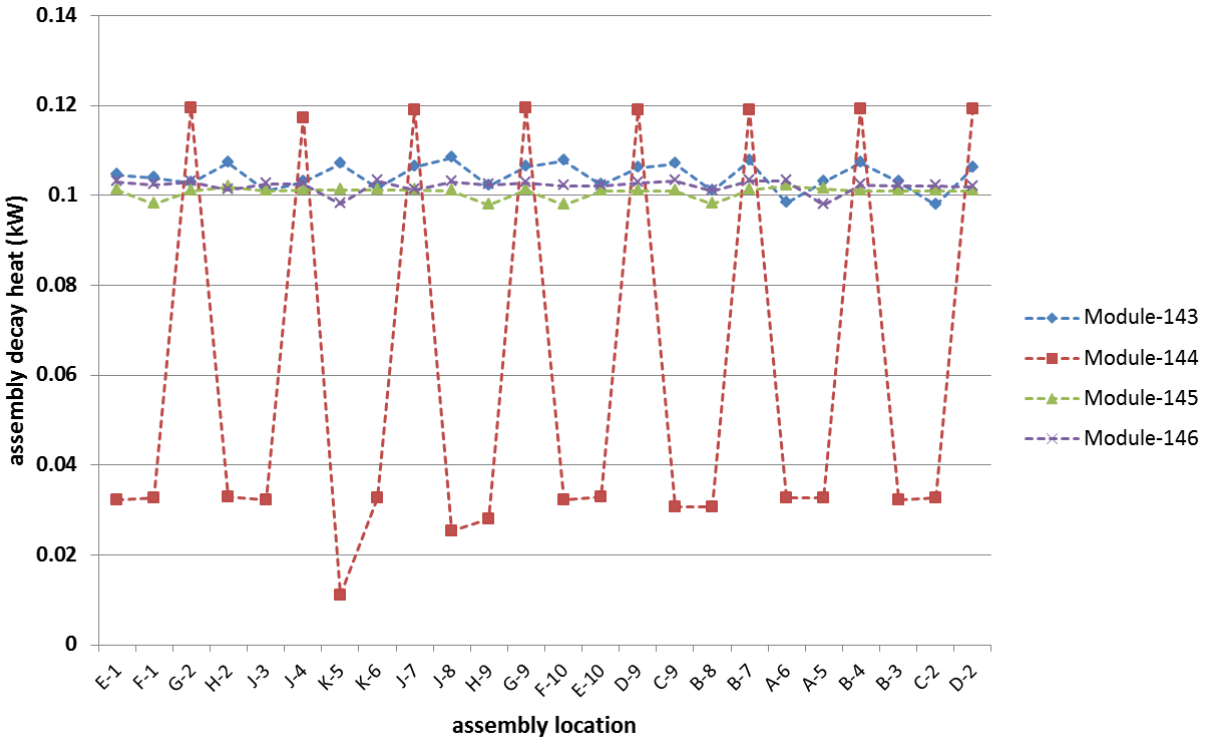

Figure 3-5. Decay Heat Values for Assemblies on Basket Periphery

Table 3-3. Summary of Decay Heat Variation Around Basket Periphery

	Maximum	Minimum	Average	Maximum deviation from average
Module 143	0.10834	0.0978	0.1042	6.1%
Module 144				
"hot" assemblies	0.1194	0.1172	0.1189	1.5%
"cold" assemblies	0.0330	0.0111	0.0297	63%
Module 145	0.1021	0.0978	0.1006	2.8%
Module 146	0.1032	0.0978	0.1020	4.1%

With the exception of Module 144, which has extremely "cold" assemblies in the paired basket end locations (e.g., E-1, F-1), the peripheral assemblies in a given basket all have nearly the same decay heat load. Even in Module 144, the variation is uniformly distributed around the circumference of the basket, and the "hot" assemblies all have nearly the same decay heat load (within 1.5% of the average). In addition to the relative uniformity of the heat load distribution, the downflow of helium gas in the spaces between the basket and the canister shell, due to natural circulation within the canister, tends to smooth out circumferential temperature gradients in the basket periphery and the canister shell.

Predicted temperature distributions around the circumference of the canister are shown in Figures 3-6 through 3-9 for the four modules, at selected axial locations along the canister height. These plots show the circumferential temperature distributions at the canister base, the canister midplane, and at the axial location of the peak outer shell temperature. As expected for the geometry and boundary conditions for this model, the circumferential variation in temperature on the canister shell is quite small. The plots in Figures 3-6 through 3-9 are for results with decay heat values from the ORIGEN modeling. Slightly higher temperatures are obtained with the decay heat values from the RG 3.54 modeling (as illustrated by the axial plots in Figures 3-1 through 3-4), but the circumferential gradients on the canister shell show essentially the same pattern.

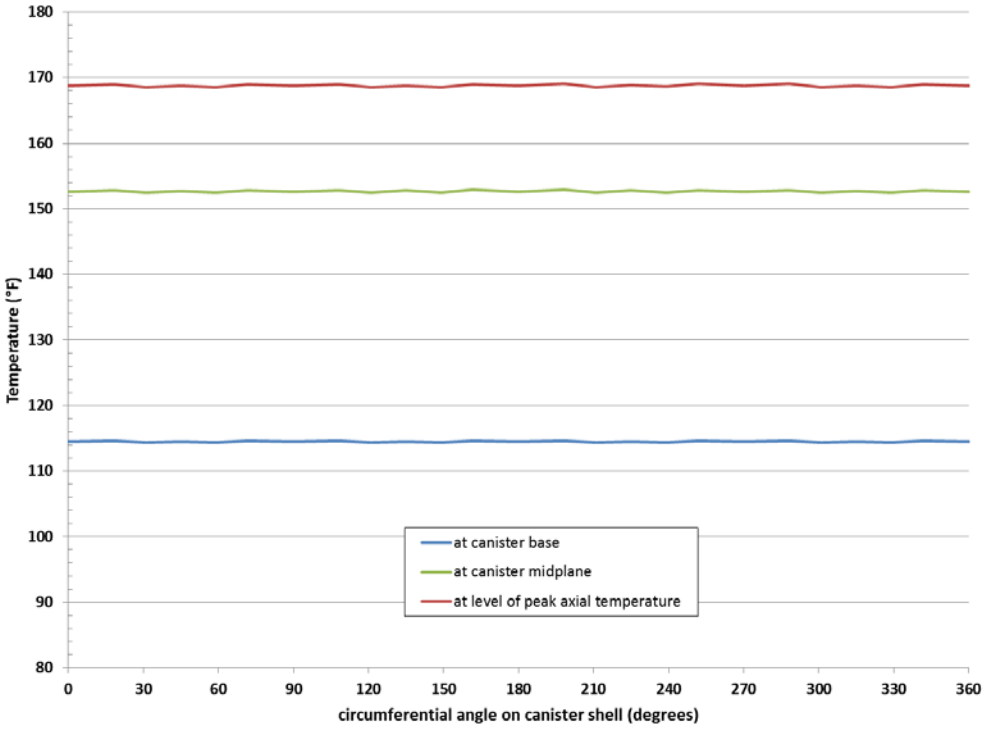

Figure 3-6. Circumferential Temperature Distribution on MPC Outer Shell for Module 143 (80°F (27°C) ambient, with decay heat values from ORIGEN modeling)

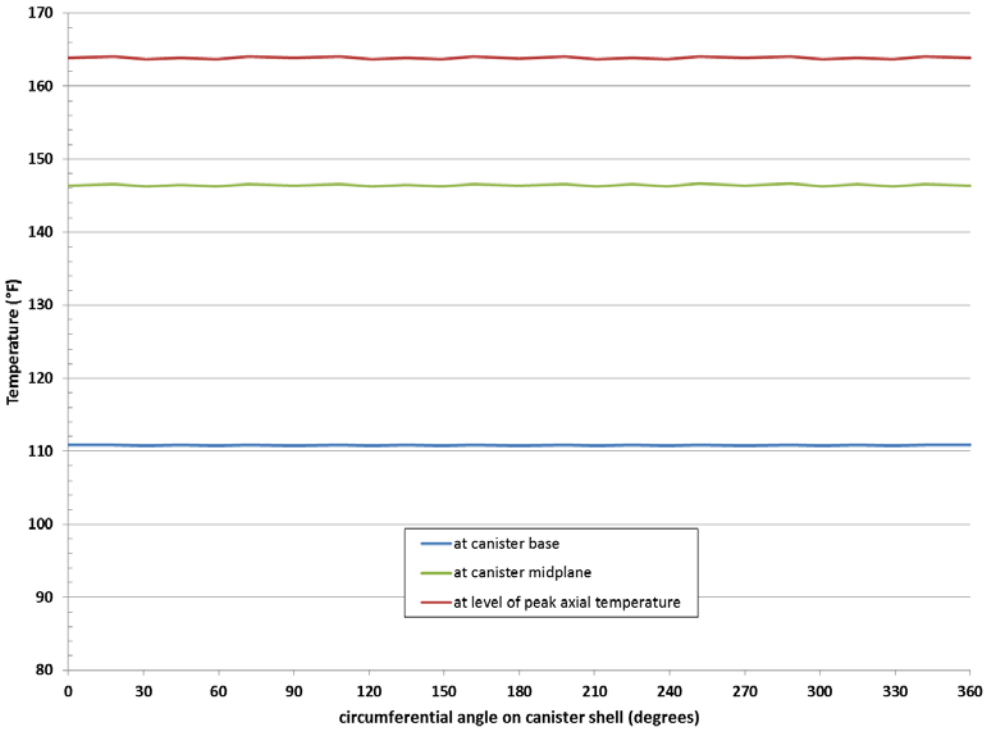

Figure 3-7. Circumferential Temperature Distribution on MPC Outer Shell for Module 144 (80°F (27°C) ambient, with decay heat values from ORIGEN modeling)

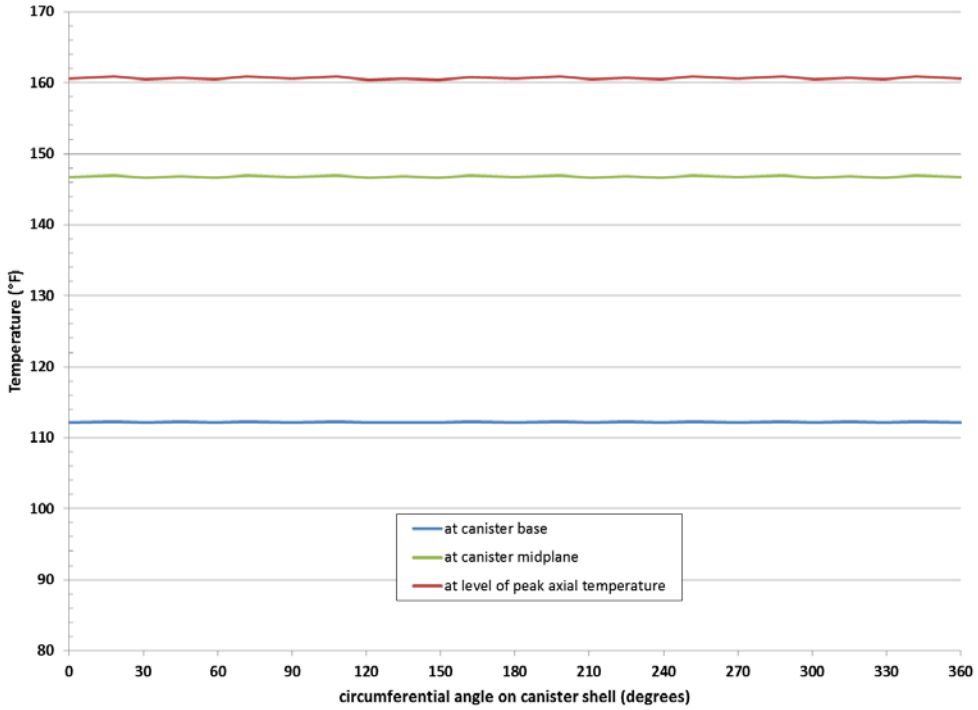

Figure 3-8. Circumferential Temperature Distribution on MPC Outer Shell for Module 145 (80°F (27°C) ambient, with decay heat values from ORIGEN modeling)

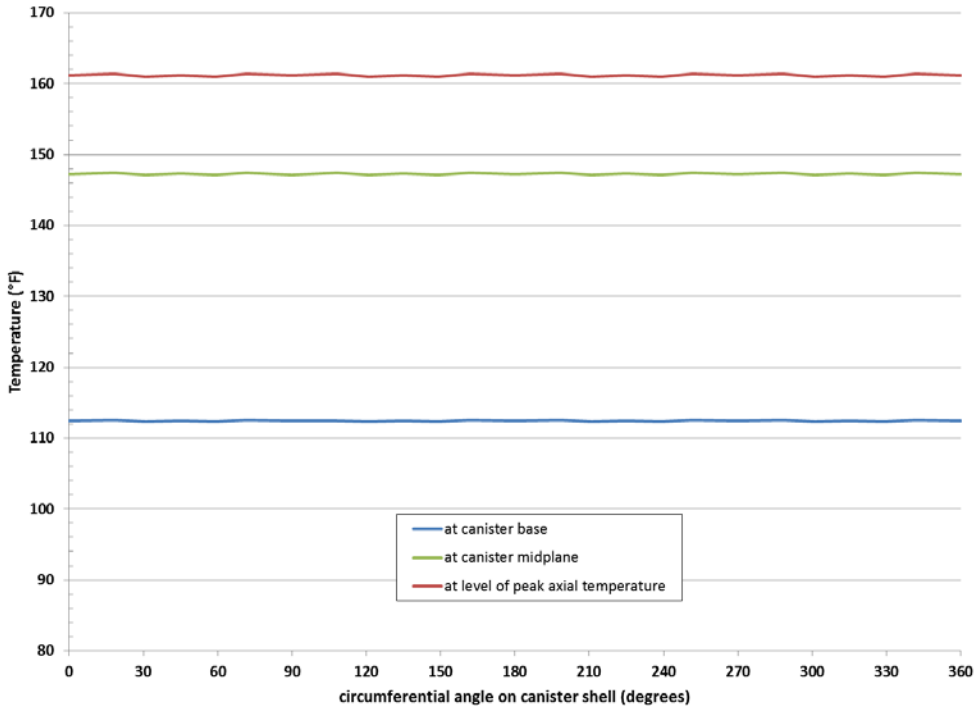

Figure 3-9. Circumferential Temperature Distribution on MPC Outer Shell for Module 146 (80°F (27°C) ambient, with decay heat values from ORIGEN modeling)

The predicted temperatures for the storage modules are sensitive to the ambient temperature, and there is some uncertainty in what the ambient temperature will be at the time of inspection. Therefore, an additional set of cases were run for Modules 144 and 145, which have been identified as the modules to be inspected. These cases provide temperature predictions for assumed daytime ambient temperatures of 90°F (32.2°C), 70°F (21.1°C), and 50°F (10°C). These calculations were performed only for the decay heat loadings based on the ORIGEN modeling, on the assumption that these are likely to be the more accurate of the two sets of projected decay heat loads for these fuel assemblies. Tables 3-4 and 3-5 show the effect of the variation in this boundary condition on the peak temperatures predicted for the two modules. Figure 3-10 shows the effect on the canister shell temperature profile in Module 144. Figure 3-11 shows the effect in Module 145.

Table 3-4. Summary of Effect of Ambient Temperature on Peak Component Temperatures, °F (°C), in the MPC

ambient temperature	fuel cladding	Fuel channel	basket plate	basket periphery	basket support	canister inner surface	canister outer surface
Module 144							
50°F (10°C)	219 (103.7)	217 (102.8)	217 (102.8)	178 (81.1)	163 (72.8)	134 (56.5)	132 (55.7)
70°F (21°C)	242 (116.6)	240 (115.6)	240 (115.6)	198 (92.4)	183 (84.2)	155 (68.1)	153 (67.4)
80°F (27°C)	254 (123.2)	252 (122.2)	252 (122.2)	209 (98.2)	194 (90.0)	165 (74.1)	164 (73.4)
90°F (32°C)	266 (129.9)	264 (128.9)	264 (128.9)	219 (104.0)	205 (95.9)	176 (80.2)	175 (79.5)
Module 145							
50°F (10°C)	215 (101.5)	213 (100.7)	213 (100.7)	174 (78.8)	161 (71.8)	134 (56.6)	133 (55.9)
70°F (21°C)	233 (111.6)	231 (110.8)	231 (110.8)	191 (88.1)	178 (81.3)	152 (66.6)	151 (65.9)
80°F (27°C)	244 (117.5)	242 (116.7)	242 (116.7)	200 (93.4)	188 (86.7)	162 (72.3)	161 (71.6)
90°F (32°C)	255 (124.1)	254 (123.2)	254 (123.2)	211 (99.3)	199 (92.7)	173 (78.5)	172 (77.8)

It is important to note that the temperatures reported here are based on steady-state calculations. This analysis does not capture the effect of diurnal temperature variation throughout the system. Thermal inertia will tend to slow the rate of change of temperatures on canister internal components in response to ambient conditions (specifically, the peak fuel cladding temperature, peak fuel channel temperature, and hottest basket plate). However, the canister shell temperature, which is directly cooled by ambient air flowing in the annulus, is expected to track local ambient fairly closely, and therefore the ambient temperature will have an effect on the measured temperatures at the time of the inspection.

Table 3-5. Summary of Effect of Ambient Temperature on Peak Component Temperatures, °F (°C), in the Overpack

ambient temperature	annulus shims	overpack inner shell	overpack concrete	overpack outer shell	overpack lid inner surface	overpack lid outer surface
Module 144						
50°F (10°C)	132 (55.5)	132 (55.5)	128 (53.4)	64 (17.5)	109 (42.7)	95 (35.2)
70°F (21°C)	153 (67.2)	153 (67.2)	149 (65.0)	84 (28.6)	109 (42.7)	95 (35.2)
80°F (27°C)	164 (73.4)	163 (73.2)	164 (73.2)	94 (34.2)	109 (42.7)	95 (35.2)
90°F (32°C)	175 (79.3)	175 (79.3)	175 (79.3)	104 (39.7)	109 (42.7)	95 (35.2)
Module 145						
50°F (10°C)	132 (55.7)	132 (55.7)	129 (53.6)	65 (18.5)	108 (42.2)	95 (35.2)
70°F (21°C)	150 (65.7)	150 (65.7)	147 (63.6)	84 (28.6)	108 (42.2)	95 (35.2)
80°F (27°C)	161 (71.4)	160 (71.4)	157 (69.4)	93 (34.1)	108 (42.2)	95 (35.2)
90°F (32°C)	172 (77.7)	172 (77.6)	168 (75.6)	103 (39.6)	108 (42.2)	95 (35.2)

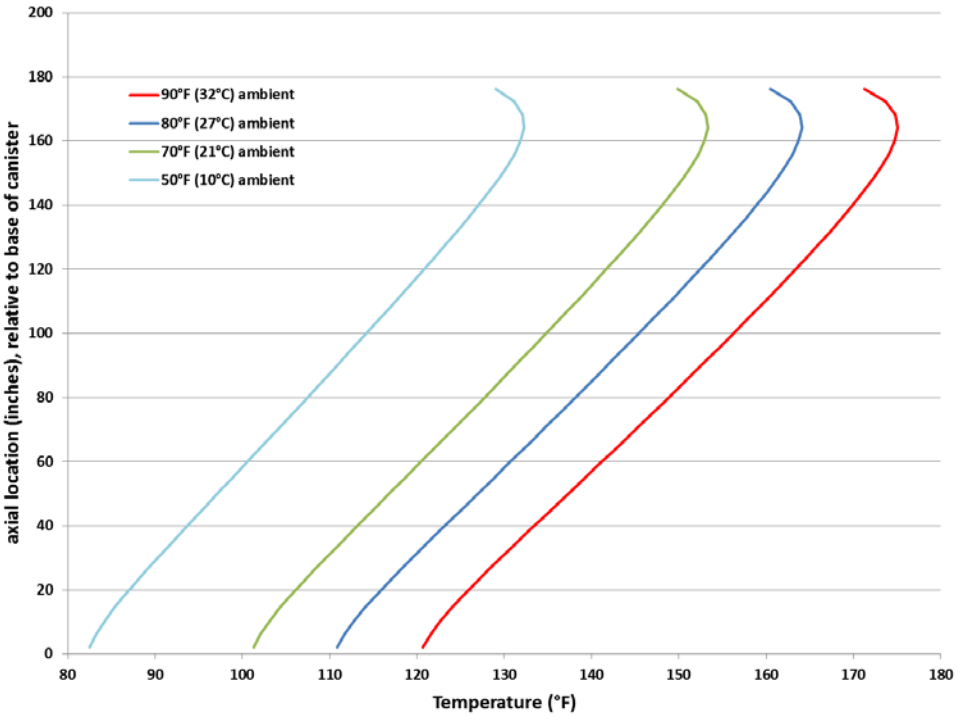

Figure 3-10. Axial Temperature Profile on MPC Outer Shell for Module 144 for a Range of Ambient Temperatures (with decay heat values from ORIGEN modeling)

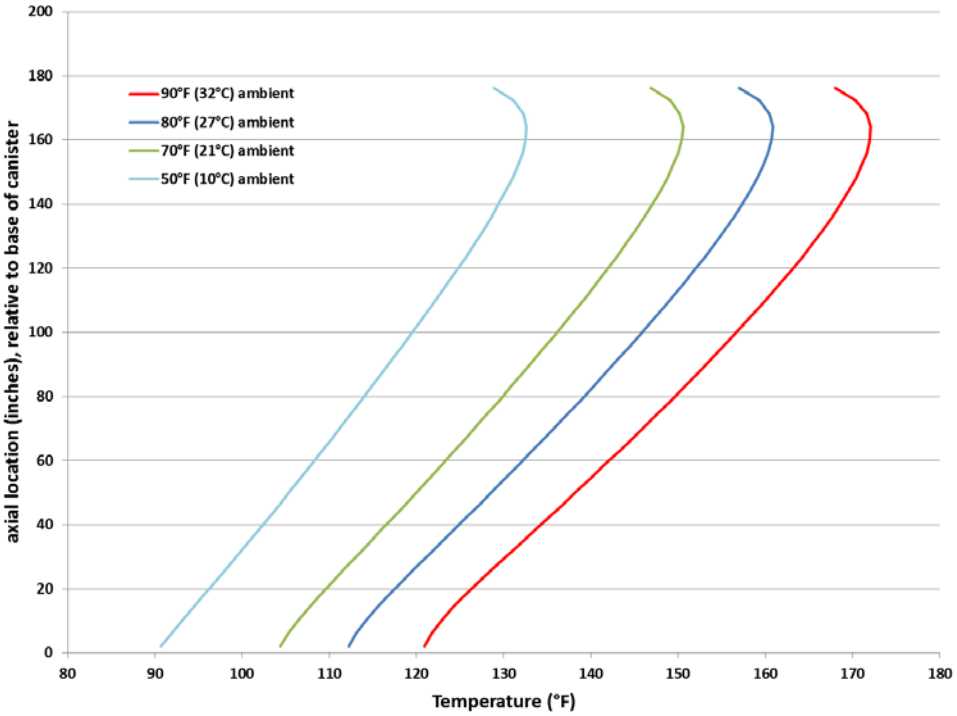

Figure 3-11. Axial Temperature Profile on MPC Outer Shell for Module 145 for Range of Ambient Temperatures (with decay heat values from ORIGEN modeling)

4.0 CONCLUSIONS

Conclusions relevant to this work will depend on the results of the inspections, and post-inspection evaluations of temperature measurements obtained in the specific modules. These will be documented in a separate follow-on report, to be issued in a timely manner after the inspection has been performed.

The current report documents pre-inspection predictions of temperatures for the four modules identified as candidates for inspection: MPC-143, -144, -145, and -146, which are HI-STORM 100S-218 Version B modules in the ISFSI at the Hope Creek Nuclear Generating Plant. These temperature predictions were obtained with detailed COBRA-SFS models of these four storage systems, with the following boundary conditions and assumptions.

- Individual assembly and canister decay heat loadings for each canister, provided by PSEG Nuclear Fuels, based on ORIGEN modeling and a parallel set of values obtained using the methodology endorsed by RG 3.54.
- Axial decay heat distributions based on typical generic profiles for BWR fuel.
- Still air, with ambient air temperature of 80°F (27°C), with additional evaluations for selected modules at 90°F (32°C), 70°F (21°C), and 50°F (10°C), to cover a range of possible conditions at the time of the inspection.

All calculations are for steady-state conditions, on the assumption that the surfaces of the module that are accessible for temperature measurements during the inspection will tend to follow ambient temperature changes relatively closely.

5.0 REFERENCES

10 CFR 71. 2003. "Packaging and Transportation of Radioactive Material." C*ode of Federal Regulations,* U.S. Nuclear Regulatory Commission, Washington D.C.

Creer JM, TE Michener, MA McKinnon, JE Tanner, ER Gilbert, and RL Goodman. 1987. *The TN-24P PWR Spent-Fuel Storage Cask: Testing and Analysis*. EPRI-NP-5128/PNL-6054, Electric Power Research Institute, Palo Alto, California.

Google. 2011. Imagery Date: 7/3/2010. Available at http://maps.google.com/maps?t=h&hl=en&ie=UTF8&ll=39.470317,-75.536537&spn=0.007669,0.013078&z=17.

Holtec International, February 13, 2010. *Final Safety Analysis Report for the HI-STORM 100 Cask System, Revision 9.* Holtec Report No. HI-2002444, USNRC Docket No. 72-1014. Holtec International, Marlton, NJ. NOTE: this document is copyrighted intellectual property of Holtec International. All rights reserved.

Lombardo NJ, JM Cuta, TE Michener, DR Rector, and CL Wheeler. 1986. *COBRA-SFS: A Thermal-Hydraulic Analysis Computer Code, Volume III: Validation Assessments*. PNL-6048 Vol. III. Pacific Northwest Laboratory, Richland, Washington.

Michener TE, DR Rector, JM Cuta, RE Dodge, and CW Enderlin. 1995. *COBRA-SFS: A Thermal-Hydraulic Code for Spent Fuel Storage and Transportation Casks*. PNL-10782, Pacific Northwest Laboratory, Richland, Washington.

NOAA 2013. " National Weather Service Forecast Office, Philadelphia/Mount Holly." Data for Wilmington, DE station at the New Castle County Airport accessed 8/21/2013 at http://www.nws.noaa.gov/climate/index.php?wfo=phi.

NRC – U.S. Nuclear Regulatory Commission. 1999. *Spent Fuel Heat Generation in an Independent Spent Fuel Storage Installation*. Regulatory Guide 3.54, Revision 1. U.S. Nuclear Regulatory Commission, Washington, D.C. Available at http://www.nrc.gov/reading-rm/doc-collections/reg-guides/fuels-materials/rg/03-054/.

Rector DR, RA McCann, UP Jenquin, CM Heeb, JM Creer, and CL Wheeler. 1986. *CASTOR-1C Spent Fuel Storage Cask Decay Heat, Heat Transfer and Shielding Analysis*. PNL-5974. Pacific Northwest Laboratory, Richland, Washington.

Sparrow EM, and LFA Azevedo. 1985. "Vertical-channel natural convection spanning between the fully-developed limit and the single-plate boundary-layer limit." I*nternational Journal of Heat and Mass Transfer*, 28(10):1847-1857.

Sparrow EM, AL Loeffler, and HA Hubbard. 1961. "Heat Transfer to Longitudinal Laminar Flow between Cylinders." *Journal of Heat Transfer*, 83:415.

Suffield SR, JM Cuta, JA Fort, BA Collins, HE Adkins, and ER Siciliano. 2012. *Thermal Modeling of NUHOMS HSM-15 and HSM-1 Storage Modules at Calvert Cliffs Nuclear Power Station ISFSI.* PNNL-21788, Pacific Northwest National Laboratory, Richland, Washington.

Turner, SE. 1989. "Uncertainty Analysis – Axial Burnup Distribution Effects," presented in *Proceedings of a Workshop on the Use of Burnup Credit in Spent Fuel Transportation Casks*, SAND-89-0018. Sandia National Laboratories, Albuquerque, New Mexico.

Appendix A

Pre-Inspection Predictions of Axial Temperature Distribution on Canister Shell

Appendix A: Pre-Inspection Predictions of Axial Temperature Distribution on Canister Shell

This appendix presents the axial temperature distributions on the MPC outer shell predicted with the COBRA-SFS models of Modules 143, 144, 145, and 146. These profiles are through the location of the peak temperature on the MPC outer shell for each configuration. The axial location in the tables is relative to the inner surface of the canister base. Results are presented for each of the four canisters in Tables A-1 through A-4. These tables contain results based on the decay heat values determined with the ORIGEN modeling and with the RG 3.54 modeling. Tables A-5 and A-6 present results for a range of ambient conditions, in Modules 144 and 145 only, which have been identified as the modules to be inspected. The results in these tables were obtained with the decay heat values from the ORIGEN modeling.

Table A-1. Canister Shell Axial Temperature Distribution: Module 143 (80°F (27°C Ambient)

Axial location (inches)	ORIGEN model: 80°F (27°C) ambient			RG 3.54 model: 80°F (27°C) ambient	
	(°F)	(°C)		(°F)	(°C)
2.05	114.6	45.9		119.4	48.6
6.10	115.5	46.4		120.5	49.1
10.15	116.7	47.1		121.9	49.9
14.20	118.1	47.8		123.5	50.8
18.25	119.6	48.7		125.2	51.8
22.30	121.2	49.5		127.0	52.8
26.35	122.8	50.4		128.9	53.8
30.40	124.4	51.3		130.8	54.9
34.45	126.1	52.3		132.7	56.0
38.50	127.7	53.2		134.6	57.0
42.55	129.4	54.1		136.5	58.1
46.60	131.0	55.0		138.5	59.1
50.65	132.7	55.9		140.4	60.2
54.70	134.3	56.8		142.3	61.3
58.75	135.9	57.7		144.2	62.3
62.80	137.5	58.6		146.0	63.4
66.85	139.1	59.5		147.9	64.4
70.90	140.7	60.4		149.8	65.4
74.95	142.3	61.3		151.6	66.4
79.00	143.8	62.1		153.4	67.5
83.05	145.4	63.0		155.2	68.5
87.15	146.9	63.8		157.0	69.5
91.20	148.4	64.7		158.8	70.4
95.25	149.9	65.5		160.6	71.4
99.30	151.4	66.3		162.3	72.4
103.35	152.9	67.1		164.0	73.4
107.40	154.3	67.9		165.7	74.3
111.45	155.7	68.7		167.4	75.2
115.50	157.1	69.5		169.1	76.2
119.55	158.5	70.3		170.7	77.1

123.60	159.8	71.0	172.3	77.9
127.65	161.1	71.7	173.9	78.8
131.70	162.4	72.4	175.4	79.6
135.75	163.5	73.1	176.8	80.4
139.80	164.7	73.7	178.2	81.2
143.85	165.7	74.3	179.4	81.9
147.90	166.7	74.8	180.6	82.6
151.95	167.6	75.3	181.7	83.2
156.00	168.3	75.7	182.7	83.7
160.05	168.8	76.0	183.3	84.1
164.10	169.0	76.1	183.6	84.2
168.15	168.7	75.9	183.3	84.0
172.20	167.4	75.2	181.8	83.2
176.25	164.9	73.8	178.8	81.6

Table A-2. Canister Shell Axial Temperature Distribution: Module 144 (80°F (27°C Ambient)

Axial location (inches)	ORIGEN model: 80°F (27°C) ambient (°F)	ORIGEN model: 80°F (27°C) ambient (°C)	RG 3.54 model: 80°F (27°C) ambient (°F)	RG 3.54 model: 80°F (27°C) ambient (°C)
2.05	110.9	43.8	115.2	46.2
6.10	111.7	44.3	116.1	46.7
10.15	112.8	44.9	117.3	47.4
14.20	114.0	45.6	118.7	48.2
18.25	115.3	46.3	120.3	49.0
22.30	116.7	47.1	121.9	49.9
26.35	118.2	47.9	123.5	50.9
30.40	119.6	48.7	125.2	51.8
34.45	121.1	49.5	127.0	52.8
38.50	122.6	50.4	128.7	53.7
42.55	124.2	51.2	130.5	54.7
46.60	125.7	52.1	132.3	55.7
50.65	127.2	52.9	134.1	56.7
54.70	128.7	53.7	135.8	57.7
58.75	130.3	54.6	137.6	58.7
62.80	131.8	55.4	139.4	59.7
66.85	133.3	56.3	141.2	60.6
70.90	134.8	57.1	142.9	61.6
74.95	136.3	58.0	144.7	62.6
79.00	137.8	58.8	146.5	63.6
83.05	139.3	59.6	148.2	64.6
87.15	140.8	60.4	150.0	65.5
91.20	142.3	61.3	151.7	66.5
95.25	143.7	62.1	153.4	67.5
99.30	145.2	62.9	155.2	68.4
103.35	146.6	63.7	156.9	69.4
107.40	148.1	64.5	158.6	70.3
111.45	149.5	65.3	160.3	71.3

115.50	150.9	66.1	162.0	72.2
119.55	152.3	66.8	163.6	73.1
123.60	153.7	67.6	165.3	74.1
127.65	155.0	68.3	166.9	75.0
131.70	156.3	69.1	168.5	75.8
135.75	157.6	69.8	170.1	76.7
139.80	158.8	70.5	171.6	77.5
143.85	160.0	71.1	173.0	78.4
147.90	161.1	71.7	174.4	79.1
151.95	162.2	72.3	175.7	79.8
156.00	163.1	72.8	176.8	80.5
160.05	163.7	73.2	177.7	80.9
164.10	164.1	73.4	178.2	81.2
168.15	163.9	73.3	178.0	81.1
172.20	162.8	72.7	176.7	80.4
176.25	160.5	71.4	174.0	78.9

Table A-3. Canister Shell Axial Temperature Distribution: Module 145 (80°F (27°C Ambient)

Axial location (inches)	ORIGEN model: 80°F (27°C) ambient			RG 3.54 model: 80°F (27°C) ambient	
	(°F)	(°C)		(°F)	(°C)
2.05	112.26	44.59		116.39	46.88
6.10	113.09	45.05		117.33	47.40
10.15	114.22	45.68		118.61	48.12
14.20	115.50	46.39		120.08	48.93
18.25	116.88	47.16		121.65	49.81
22.30	118.33	47.96		123.30	50.72
26.35	119.80	48.78		124.99	51.66
30.40	121.30	49.61		126.70	52.61
34.45	122.81	50.45		128.42	53.57
38.50	124.31	51.28		130.14	54.52
42.55	125.82	52.12		131.87	55.48
46.60	127.31	52.95		133.58	56.43
50.65	128.80	53.78		135.29	57.38
54.70	130.28	54.60		136.99	58.33
58.75	131.75	55.42		138.67	59.26
62.80	133.20	56.22		140.35	60.19
66.85	134.64	57.02		142.01	61.11
70.90	136.07	57.82		143.65	62.03
74.95	137.48	58.60		145.28	62.93
79.00	138.88	59.38		146.90	63.83
83.05	140.26	60.15		148.50	64.72
87.15	141.63	60.91		150.08	65.60
91.20	142.98	61.66		151.65	66.47
95.25	144.32	62.40		153.21	67.34
99.30	145.64	63.13		154.74	68.19
103.35	146.94	63.86		156.26	69.03
107.40	148.22	64.57		157.76	69.86

111.45	149.48	65.27	159.23	70.68
115.50	150.71	65.95	160.67	71.49
119.55	151.91	66.62	162.09	72.27
123.60	153.08	67.27	163.47	73.04
127.65	154.21	67.89	164.80	73.78
131.70	155.29	68.49	166.08	74.49
135.75	156.32	69.07	167.31	75.17
139.80	157.28	69.60	168.46	75.81
143.85	158.18	70.10	169.54	76.41
147.90	159.00	70.55	170.53	76.96
151.95	159.72	70.96	171.42	77.45
156.00	160.32	71.29	172.16	77.87
160.05	160.74	71.52	172.69	78.16
164.10	160.85	71.58	172.87	78.26
168.15	160.47	71.37	172.47	78.04
172.20	159.31	70.73	171.14	77.30
176.25	157.03	69.46	168.45	75.81

Table A-4. Canister Shell Axial Temperature Distribution: Module 146 (80°F (27°C Ambient)

Axial location (inches)	ORIGEN model: 80°F (27°C) ambient (°F)	(°C)		RG 3.54 model: 80°F (27°C) ambient (°F)	(°C)
2.05	112.49	44.72		116.68	47.04
6.10	113.33	45.18		117.62	47.57
10.15	114.46	45.81		118.91	48.28
14.20	115.76	46.53		120.39	49.10
18.25	117.15	47.31		121.98	49.99
22.30	118.60	48.11		123.64	50.91
26.35	120.09	48.94		125.34	51.86
30.40	121.60	49.78		127.07	52.82
34.45	123.12	50.62		128.80	53.78
38.50	124.64	51.46		130.54	54.75
42.55	126.15	52.31		132.28	55.71
46.60	127.66	53.14		134.01	56.67
50.65	129.16	53.98		135.73	57.63
54.70	130.65	54.81		137.44	58.58
58.75	132.13	55.63		139.14	59.52
62.80	133.59	56.44		140.83	60.46
66.85	135.04	57.25		142.50	61.39
70.90	136.48	58.04		144.16	62.31
74.95	137.90	58.84		145.80	63.22
79.00	139.31	59.62		147.43	64.13
83.05	140.70	60.39		149.04	65.02
87.15	142.08	61.16		150.64	65.91
91.20	143.44	61.91		152.22	66.79
95.25	144.79	62.66		153.78	67.66
99.30	146.12	63.40		155.33	68.52
103.35	147.43	64.13		156.86	69.37

107.40	148.72	64.84	158.37	70.20
111.45	149.99	65.55	159.85	71.03
115.50	151.23	66.24	161.31	71.84
119.55	152.44	66.91	162.73	72.63
123.60	153.61	67.56	164.12	73.40
127.65	154.75	68.19	165.46	74.14
131.70	155.84	68.80	166.75	74.86
135.75	156.87	69.37	167.98	75.55
139.80	157.84	69.91	169.15	76.19
143.85	158.74	70.41	170.23	76.79
147.90	159.56	70.87	171.22	77.35
151.95	160.29	71.27	172.11	77.84
156.00	160.89	71.61	172.86	78.26
160.05	161.31	71.84	173.39	78.55
164.10	161.42	71.90	173.57	78.65
168.15	161.03	71.69	173.16	78.42
172.20	159.86	71.03	171.81	77.67
176.25	157.55	69.75	169.10	76.17

Table A-5. Canister Shell Axial Temperature Distributions for Module 144 for a Range of Ambient Temperatures

Axial location (inches)	ORIGEN model							
	90°F (32°C) ambient		80°F (27°C) ambient		70°F (21°C) ambient		50°F (10°C) ambient	
	(°F)	(°C)	(°F)	(°C)	(°F)	(°C)	(°F)	(°C)
2.05	120.70	49.28	110.9	43.8	101.29	38.49	82.5	28.1
6.10	121.55	49.75	111.7	44.3	102.04	38.91	83.2	28.5
10.15	122.66	50.37	112.8	44.9	103.08	39.49	84.2	29.0
14.20	123.92	51.07	114.0	45.6	104.25	40.14	85.3	29.6
18.25	125.29	51.83	115.3	46.3	105.53	40.85	86.5	30.3
22.30	126.73	52.63	116.7	47.1	106.88	41.60	87.8	31.0
26.35	128.22	53.46	118.2	47.9	108.28	42.38	89.1	31.7
30.40	129.75	54.30	119.6	48.7	109.71	43.17	90.4	32.5
34.45	131.30	55.16	121.1	49.5	111.16	43.98	91.8	33.2
38.50	132.86	56.03	122.6	50.4	112.63	44.80	93.2	34.0
42.55	134.43	56.91	124.2	51.2	114.11	45.62	94.6	34.8
46.60	136.00	57.78	125.7	52.1	115.59	46.44	96.0	35.5
50.65	137.58	58.66	127.2	52.9	117.07	47.26	97.4	36.3
54.70	139.15	59.53	128.7	53.7	118.55	48.09	98.8	37.1
58.75	140.72	60.40	130.3	54.6	120.04	48.91	100.2	37.9
62.80	142.29	61.27	131.8	55.4	121.51	49.73	101.6	38.6
66.85	143.84	62.14	133.3	56.3	122.99	50.55	103.0	39.4
70.90	145.39	63.00	134.8	57.1	124.46	51.36	104.4	40.2
74.95	146.94	63.85	136.3	58.0	125.92	52.18	105.7	41.0
79.00	148.47	64.71	137.8	58.8	127.38	52.99	107.1	41.7
83.05	150.00	65.55	139.3	59.6	128.83	53.79	108.5	42.5
87.15	151.52	66.40	140.8	60.4	130.27	54.60	109.9	43.3
91.20	153.02	67.24	142.3	61.3	131.71	55.40	111.3	44.0
95.25	154.52	68.07	143.7	62.1	133.15	56.19	112.6	44.8
99.30	156.01	68.89	145.2	62.9	134.57	56.98	114.0	45.5

103.35	157.49	69.72	146.6	63.7	135.99	57.77	115.3	46.3
107.40	158.95	70.53	148.1	64.5	137.40	58.55	116.7	47.0
111.45	160.40	71.33	149.5	65.3	138.80	59.33	118.0	47.8
115.50	161.83	72.13	150.9	66.1	140.18	60.10	119.4	48.5
119.55	163.25	72.91	152.3	66.8	141.55	60.86	120.7	49.3
123.60	164.64	73.69	153.7	67.6	142.90	61.61	122.0	50.0
127.65	166.00	74.44	155.0	68.3	144.23	62.35	123.3	50.7
131.70	167.33	75.18	156.3	69.1	145.53	63.07	124.6	51.4
135.75	168.62	75.90	157.6	69.8	146.80	63.78	125.8	52.1
139.80	169.86	76.59	158.8	70.5	148.03	64.46	127.0	52.8
143.85	171.04	77.25	160.0	71.1	149.21	65.12	128.2	53.4
147.90	172.16	77.86	161.1	71.7	150.33	65.74	129.3	54.0
151.95	173.17	78.43	162.2	72.3	151.36	66.31	130.3	54.6
156.00	174.05	78.92	163.1	72.8	152.25	66.81	131.2	55.1
160.05	174.71	79.29	163.7	73.2	152.95	67.19	131.9	55.5
164.10	175.03	79.46	164.1	73.4	153.31	67.39	132.3	55.7
168.15	174.80	79.33	163.9	73.3	153.14	67.30	132.1	55.6
172.20	173.68	78.71	162.8	72.7	152.11	66.73	131.2	55.1
176.25	171.29	77.38	160.5	71.4	149.88	65.49	129.1	53.9

Table A-6. Canister Shell Axial Temperature Distributions for Module 145 for a Range of Ambient Temperatures

axial location (inches)	ORIGEN model							
	90°F (32°C) ambient		80°F (27°C) ambient		70°F (21°C) ambient		50°F (10°C) ambient	
	(°F)	(°C)	(°F)	(°C)	(°F)	(°C)	(°F)	(°C)
2.05	120.90	49.39	112.26	44.59	104.42	40.23	90.74	32.63
6.10	121.71	49.84	113.09	45.05	105.32	40.73	91.88	33.27
10.15	122.86	50.48	114.22	45.68	106.45	41.36	93.13	33.96
14.20	124.20	51.22	115.50	46.39	107.71	42.06	94.40	34.67
18.25	125.66	52.03	116.88	47.16	109.04	42.80	95.68	35.38
22.30	127.20	52.89	118.33	47.96	110.41	43.56	96.95	36.08
26.35	128.78	53.76	119.80	48.78	111.80	44.33	98.21	36.78
30.40	130.38	54.66	121.30	49.61	113.20	45.11	99.46	37.48
34.45	132.00	55.56	122.81	50.45	114.60	45.89	100.70	38.17
38.50	133.62	56.46	124.31	51.28	116.00	46.67	101.93	38.85
42.55	135.24	57.36	125.82	52.12	117.40	47.45	103.15	39.53
46.60	136.86	58.25	127.31	52.95	118.79	48.22	104.36	40.20
50.65	138.46	59.14	128.80	53.78	120.18	48.99	105.56	40.87
54.70	140.05	60.03	130.28	54.60	121.55	49.75	106.76	41.53
58.75	141.63	60.91	131.75	55.42	122.91	50.51	107.94	42.19
62.80	143.19	61.77	133.20	56.22	124.26	51.26	109.12	42.84
66.85	144.74	62.63	134.64	57.02	125.61	52.00	110.29	43.49
70.90	146.27	63.48	136.07	57.82	126.94	52.74	111.45	44.14
74.95	147.78	64.32	137.48	58.60	128.25	53.47	112.60	44.78
79.00	149.28	65.15	138.88	59.38	129.56	54.20	113.74	45.41
83.05	150.75	65.97	140.26	60.15	130.85	54.92	114.88	46.04
87.15	152.21	66.78	141.63	60.91	132.13	55.63	116.00	46.67
91.20	153.65	67.58	142.98	61.66	133.40	56.33	117.12	47.29

95.25	155.06	68.37	144.32	62.40	134.66	57.03	118.23	47.91
99.30	156.46	69.14	145.64	63.13	135.90	57.72	119.34	48.52
103.35	157.83	69.91	146.94	63.86	137.13	58.41	120.43	49.13
107.40	159.18	70.66	148.22	64.57	138.34	59.08	121.51	49.73
111.45	160.51	71.39	149.48	65.27	139.54	59.74	122.58	50.32
115.50	161.80	72.11	150.71	65.95	140.71	60.39	123.63	50.91
119.55	163.05	72.81	151.91	66.62	141.85	61.03	124.67	51.48
123.60	164.27	73.48	153.08	67.27	142.97	61.65	125.68	52.04
127.65	165.44	74.13	154.21	67.89	144.05	62.25	126.66	52.59
131.70	166.55	74.75	155.29	68.49	145.09	62.83	127.61	53.12
135.75	167.61	75.34	156.32	69.07	146.08	63.38	128.52	53.62
139.80	168.59	75.88	157.28	69.60	147.02	63.90	129.39	54.10
143.85	169.50	76.39	158.18	70.10	147.89	64.39	130.19	54.55
147.90	170.32	76.84	159.00	70.55	148.70	64.83	130.94	54.97
151.95	171.04	77.24	159.72	70.96	149.41	65.23	131.60	55.33
156.00	171.62	77.57	160.32	71.29	150.01	65.56	132.16	55.64
160.05	172.01	77.78	160.74	71.52	150.43	65.79	132.54	55.86
164.10	172.08	77.82	160.85	71.58	150.56	65.87	132.63	55.91
168.15	171.64	77.58	160.47	71.37	150.21	65.67	132.25	55.69
172.20	170.40	76.89	159.31	70.73	149.09	65.05	131.10	55.05
176.25	167.99	75.55	157.03	69.46	146.87	63.82	128.84	53.80